Министерство образования Республики Беларусь
Учреждение образования
«Полоцкий государственный университет»

Н. Н. Попок
С. В. Дербуш
А. Н. Попок

ИОННЫЕ ИСТОЧНИКИ: ВИДЫ, КОНСТРУКЦИИ, ПРИМЕНЕНИЕ

Пособие для студентов и магистрантов
машиностроительных специальностей

ION SOURCES: VARIETY, CONSTRUCTION, APPLICATION

Manual for students and masters
of engineering specialities

Новополоцк
Полоцкий государственный университет
2017

УДК 621.793(075.8)
ББК 34.58я73
П41

Рекомендовано к изданию методической комиссией
факультета машиностроения и автомобильного транспорта
в качестве пособия (протокол № 12 от 12 декабря 2016 г.)

РЕЦЕНЗЕНТЫ:
д-р физ.-мат. наук, доц.,
директор Физико-технического института НАН Беларуси
В. Г. ЗАЛЕССКИЙ;
канд. техн. наук, доц. зав. каф. автомобильного транспорта
Полоцкого государственного университета Т. В. ВИГЕРИНА

Попок, Н. Н.

П41 Ионные источники: виды, конструкции, применеие = Ion sources: variety, construction, application : пособие для студентов и магистрантов машиностроит. специальностей / Н. Н. Попок, С. В. Дербуш, А. Н. Попок. – Новополоцк : Полоц. гос. ун-т, 2017. – 72 с.

ISBN 978-985-531-559-0.

Рассмотрены основные виды и конструкции ионных источников, их применение. Приведены результаты собственных научных исследований авторов по ионно-лучевой обработке материалов и рекомендации по проведению учебно-исследовательской лабораторной работы.

Для студентов и магистрантов машиностроительных специальностей.

УДК 621.793(075.8)
ББК 34.58я73

ISBN 978-985-531-559-0

FOREWORD

During the design of a particle accelerator, the origin and identity of the particle is often treated as a mathematical fiction instead of an entity that must be produced at the beginning of the acceleration process. In many cases the source of the particles must be made to fit around the design instead of being taken into consideration at an early stage. However, accelerators are not the only users of particle beams. Applications range from providing beams of hundreds of Amperes for fusion applications, nanoamperes for microprobe trace analysis, broad beams for ion implantation, space thrusters, industrial polymerisation, food sterilisation, to medical, military and accelerator applications. The types of particles involved are equally as numerous and are limited only by the availability of a suitable source. Let's consider a selection of ion source types which can be found.

Selection of types of ion source

Surface ionisation	Plasma beam
Field ionisation	Duoplasmatron
Sputter	Hollow cathode
Laser	Pigatrons
Electron beam ionisation	Multifilament
Arc discharge	Cyclotron resonance
Multipole confinement	Surface plasma
Pennings	Magnetrons
Charge exchange	RF plasma

As can be seen, the field is vast and can not be covered in a paper like this. Instead we will cover some of those sources which are of interest to the accelerator field.

In any gaseous discharge, both negatively and positively charged particles exist in approximately equal proportions along with un-ionized neutrals, i.e. they form a plasma. For a simple ion source, it is only necessary to extract the ion from the plasma and then to accelerate it. However, a reasonable current with good beam qualities is usually needed and the objective of source design is to optimise the desired ion yield and beam quality.

LECTURE COURSE

1. ELEMENTARY ION SOURCES

1.1. Introduction

This chapter is a first primer, or very basic introduction to ion sources. Here we discuss the most fundamental features of ion sources. We introduce the terminology, describe the difference between an ***ion source*** and a ***plasma source***, the specific ingredients of an ion source, and the important features that go together to make an elementary ion source. With this background we conceptually design a simple ion source and consider the peripheral supporting power supplies. Finally, we discuss the example of a specific kind of ion source, noting how its features are simply the hardware embodiments of the principles we have previously outlined.

1.2. Terminology

In the wider scientific community there is often confusion between the terms ***plasma source*** and ***ion source***. Since a plasma is an assemblage of ions and electrons, it may seem reasonable that a device that generates a plasma might equally well be called an ion generator or ion source. While perhaps logically correct, this is not how the terminology has evolved. In conventional parlance, by ion source we mean ion beam source or ion beam generator. Most (but not all) ion sources are plasma-based in the sense that they contain a plasma as an essential part; the plasma source, which constitutes an important part of the ion source, is used to produce ions that are then formed into a more-or-less energetic ion beam.

With minimal loss of generality, we might say that the ions formed by a plasma source usually possess little directed energy – the ion drift energy is zero or at least small compared to the mean thermal ion energy. On the other hand, the ions formed by an ion source usually possess significant directed energy – the ions are in the form of a beam and have a drift energy that is large compared to the mean thermal energy. There is in concept a gradual transition from the plasma source regime to the ion source regime, and in the intermediate regime there is a gray or fuzzy area that can be thought of either way – quite productively, in fact. Consider the case of a plasma that is formed in such a way as to possess substantial drift, perhaps by making use of the Hall effect (i.e., the $\boldsymbol{j} \times \boldsymbol{B}$ force) to accelerate the plasma as a whole at the same time as it is formed. We can view this either as a plasma with high drift velocity, or as a relatively

low energy ion beam embedded in its own background sea of cold electrons. This approach can be used as a technique for forming low energy ion beams, and the background electrons in fact serve the useful function of space-charge-neutralization and inhibition of space-charge blow-up of the beam. A device that produces a streaming plasma of this general kind is often called a ***plasma gun***.

In the usual case, then, the *ion source contains a plasma source as its most essential component*. By one means or another, plasma is formed within the heart of the ion source, and the hardware and electronics needed to form the plasma are some of the key parts of the overall ion source setup. The properties and features of the plasma determine to a large extent the kind of ion beam that is produced. For example, if the need is for a high current, repetitively-pulsed, small diameter beam of xenon ions, then the plasma source that forms the heart of the ion source should be a high density, repetitively-pulsed, gaseous (xenon) plasma source of modest size. The ion beam is formed from the plasma by an electrode system – specially shaped metal electrodes to which voltages are applied. The plasma is located on one side of the electrode structure, and the ion beam is formed and transported originating from the other side. A misnomer has evolved in that this beam-forming electrode system is commonly called the extractor, and the grids are sometimes called the extraction electrodes, implying that ions are extracted from the plasma by the electrodes. Actually ions are not "pulled out" of the plasma at all; rather, they flow from the plasma to the electrode system at a rate quite independent of the extractor voltage, and are subsequently accelerated by the extractor into an energetic beam. Thus the term accelerator is also sometimes used to refer to the beam-forming electrode system. Nevertheless, the term extractor is very widely used, and we will continue to use this familiar terminology here while keeping in mind that the word is not strictly correct and is of historical origin.

1.3. The Quintessential Ion Source

The ion source that we've conceptually developed so far thus consists of a ***plasma source*** and an ***extractor***. Ions are formed in an appropriate kind of plasma source located within the ion source, and an electrode system, usually called the extractor, is located so that some of the plasma flows toward it. Voltages, often quite high voltages, are applied to the various electrodes of the extractor system and the ions that flow toward it are accelerated and formed into an energetic ion beam. The beam emerges from the extractor and enters the downstream region where the ion beam application awaits it. Our quintessential ion source at its present embryonic level can be represented in a much-oversimplified way as shown in Figure 1.1.

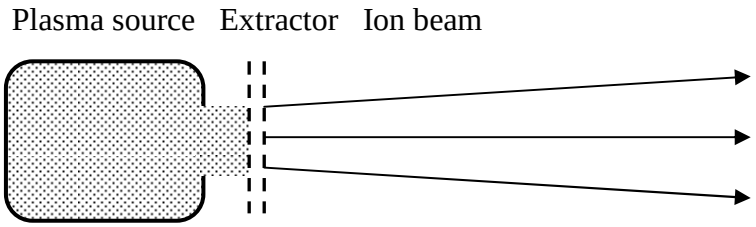

Figure 1.1. The elemental ion source: a plasma source for ion production and an electrode system for forming the ions into a beam

Now consider the way in which voltages must be applied in order to form the wanted beam. We recognize that the plasma formation system will itself require its own electrical support system. Plasmas are made electrically and they are often confined magnetically. The electrical power supplies, solenoid supplies, control systems, monitoring electronics, etc, that are required just for the plasma part of the ion source constitute an important and usually sophisticated part of the overall electrical/electronics system. But our evolving conceptual development is not at this stage yet. Firstly we need to consider the way in which the plasma source and the extractor should be biased. Figure 1.1 can be developed further by adding to it the electric potentials of its components and the downstream application region. Keeping in mind that all ion sources operate in a low pressure environment and that thus all laboratory ion sources are operated within a vacuum system of some kind, we can consider the downstream application region to be a metal vacuum chamber. Let us allow the plasma source to be fixed at a potential V_{ps} with respect to ground, the extraction system at potential V_{ext}, and the space within the downstream vacuum chamber at potential V_{ch}. The extractor system may be composed of multiple electrodes at various potentials V_{ext1}, V_{ext2}, etc, and we carry this along in concept; our conclusions will not be changed by this generalization. We can draw a schematic of the potential distribution of the complete region as a function of distance along the system, all the way from within the plasma source where the ions are born to the downstream region where the ions are used, as shown in Figure 1.2.

Considering our ions to be positively charged with charge state (or ionization state) $Q+$, then the downstream ion energy, i.e., the energy of the beam ions, is given by

$$Ei = eQ(V_{ps} - V_{ch}), \tag{1.1}$$

where e is the (magnitude of the) electronic charge. Let us now assume that the downstream vacuum chamber is at ground potential, as is overwhelmingly the usual case. Then $V_{ch} = 0$ and

$$Ei = eQV_{ps}, \tag{1.2}$$

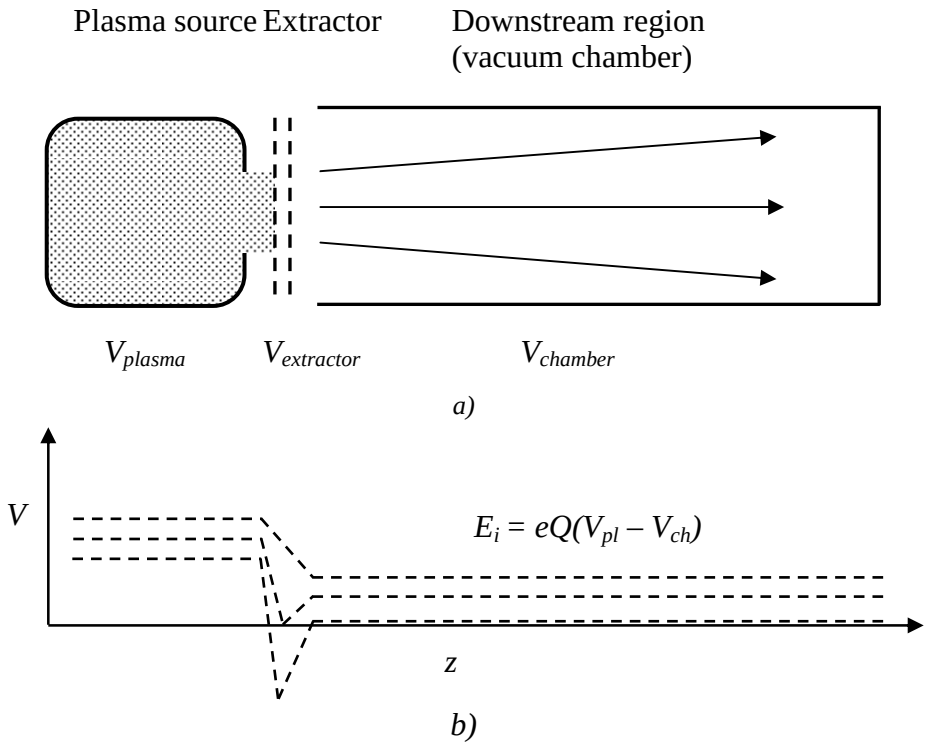

Figure 1.2. The elemental ion source: a) schematic image of the source;
b) dependency the potential variation from plasma source to downstream region

That is, the ion beam energy (energy of the ions in the beam) is determined solely by the ion charge state and the voltage to which the plasma source is biased. Although this is clear when we consider the potential diagram above, it is important to point out. It is a misconception, not infrequently assumed by beginning ion source users, that a simple ion source can be made by placing a negatively biased grid in front of a plasma source that is at ground potential, with the ion energy then determined by the grid voltage. We see from the above that in order to form a beam of ions of energy E_i, the plasma source must be held at voltage $Vps = E_i/eQ$. If the ions are positively charged, as is commonly the case, then the plasma source must be held at positive potential, and for negative ions conversely the plasma source should be negative. For singly charged positive ions, and if we permit loose substitution between the use of electron volts (*eV*) and volts (*V*), then the plasma source bias voltage, which we can also call the ion source bias voltage, is equal to the ion energy. In order to form a beam of singly-ionized, positively-charged ions of energy (say) 20 *keV*, we must bias the ion source to a voltage of +20 *kV*. (See Ref. [1] for an unusual alternative approach, however). Adding these features, our elementary ion source evolves a little further and can be represented schematically as shown in Figure 1.3.

In Figure 1.3 we have included a high voltage power supply that provides the bias voltage necessary for the system to operate in the way described above. For simplicity we continue to assume positive ions. The primary high voltage supply is often called the extractor supply, or perhaps more correctly the accelerator supply. It determines the potential drop through which the ions fall – their acceleration voltage. Thus the final ion energy is given by the extraction voltage as

$$Ei = eQV_{ext}, \tag{1.3}$$

which is the same as Eq. (1.2) if $V_{ps} = V_{ext}$. Actually, although this is usually a good approximation it is not exactly correct. The plasma potential (defined as the potential of the plasma with respect to the wall of the chamber that contains it) is usually of the order of 3kTe, and the electron temperature Te is often only a few *eV*.

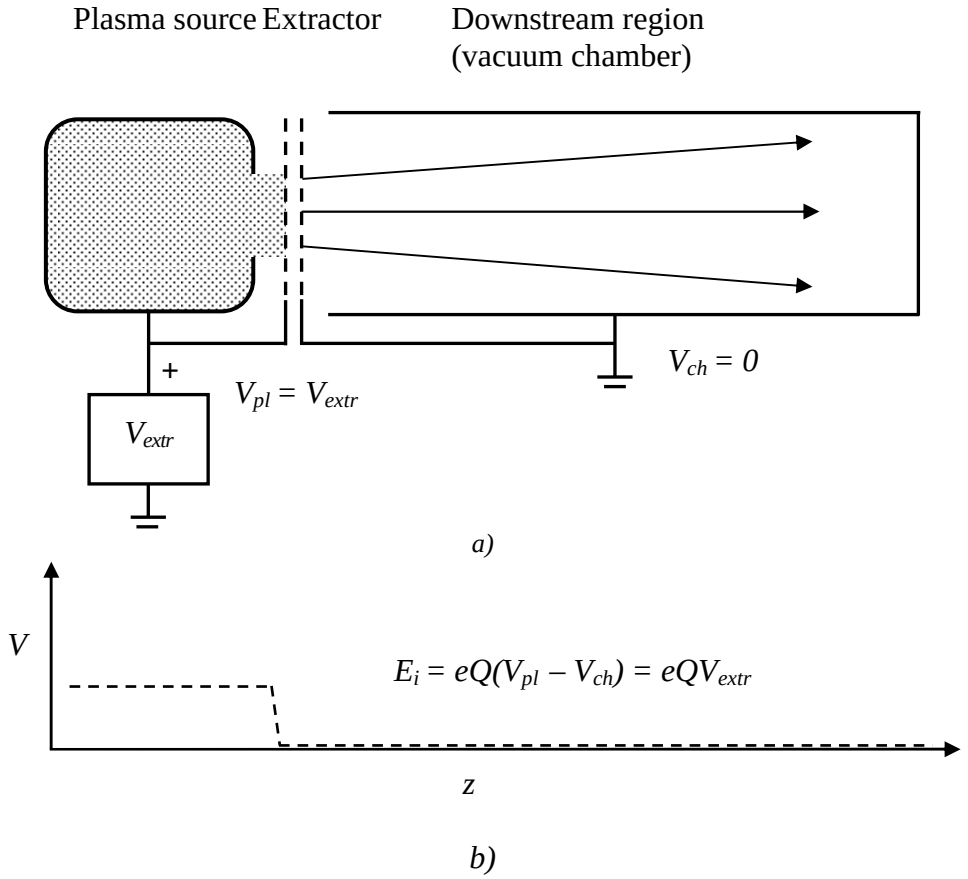

Figure 1.3. The elemental ion source: a) the first extractor grid more-or-less incorporated into the plasma chamber structure, b) the downstream space (vacuum chamber) at ground potential

Thus the plasma potential V_{pl} is typically of order +10 *V*, and so can well be neglected compared to an extraction voltage of some or many kilovolts. Nevertheless, for the case of low energy ion sources, and for the case when we

need to account for the ion beam energy with good precision, we need to keep in mind that the ions formed within the plasma source are born at a potential that is different from the plasma source bias voltage by the plasma potential.

1.4. Ion Beam Formation

The ion beam is formed from the plasma ions by an electrode system to which voltages are applied, commonly called the extractor. The plasma physics of beam formation is actually quite complicated. Here we outline the extraction process in great simplicity, just enough to let us proceed with our conceptual development of the elementary ion source. The extractor can take many different forms, consisting of from one to as many as five or six different electrodes, and with widely different geometries. In all cases the object is to accept into the extractor the plasma flux that is presented to it from the main body of plasma, and to accelerate the ions into a more-or-less tight beam.

Note that in a quite real sense, the plasma flux that the extractor sees is the loss flux from the plasma – the ions that are available for beam-forming are not those that are confined within the plasma system but those that are lost from the confinement system. Sometimes it can be that the parameters of the ion loss flux, that is of the ions that are formed into a beam, are rather different from the parameters of the ions that are well-confined within the plasma. For example, the charge state distribution or energy distribution of the beam ions might be different from the plasma ions if the mechanism of ion loss from the plasma is charge-state dependent or energy dependent. In any case, plasma flows or diffuses to the extractor region from the main plasma region. Reasonably, the extractor geometry is mainly determined by the size and shape of the wanted beam. If we wish to form a small diameter beam of circular cross-section, then the extractor should contain just one small hole; we call this a single-aperture design. If a broad beam is needed, then the extractor should be comprised of an array of many apertures – a multi-aperture extractor. Each aperture might be a small circular hole or there may be many slit apertures making use of rail electrodes.

Sometimes the electrodes are shaped in a way reminiscent of the Pierce electrode design [2] used for optimizing the formation of high quality electron beams, so as to tailor the precise field shape for optimal ion beam formation. In the simplest case, two separate electrodes are used. The first electrode is in contact with the plasma and is maintained at the positive (for positively charged ions) high voltage that is the extraction potential, and the second electrode is fixed at ground potential. Thus the ion-accelerating electric field is located between the electrodes of the extractor. The first electrode is often called the

plasma electrode and the second the ground electrode. Often the electrodes are called grids, especially (but not only) if they are of multi-aperture design and thus grid-like in appearance. Sometimes actual wire meshes are used for the extractor grids and in this case the terminology is of course very appropriate. Wire meshes are certainly a simple and low cost approach, and they can work satisfactorily if the ion source and ion beam requirements are not rigorous or demanding; but more commonly metal electrodes of some precision are used. It is possible to do away with the plasma grid and to use a single electrode only [3, 4]. In this case the plasma is maintained at high voltage as usual, and a high voltage sheath is formed between the plasma and the ground electrode; then the accelerating electric field is the field formed within the plasma sheath itself. This approach is rather uncommon in the West and seems to have been used more in Russia. Often a three-electrode extractor design is used, with the new electrode inserted between the plasma grid and the ground grid and biased to a relatively low negative voltage. The function of the middle grid is to inhibit the back-flow of electrons into the ion source from the downstream region, and so it is often call the suppressor grid. This three-grid configuration is also called an accel-decel extractor system, because ions are accelerated in the first gap and decelerated in the second gap. When the extraction voltage is very high, perhaps several hundred kilovolts or even up to a megavolt, then additional electrodes are often used whose purpose is primarily to provide a defined grading of the very high electric field so as to be able to hold off the high voltage without breakdown. Note that in all cases the final or outermost grid is maintained at ground potential; it is important that the last electrode of the system be at the same potential as the downstream region. Extractor systems of the kind we have discussed can be represented schematically as shown in Figure 1.4.

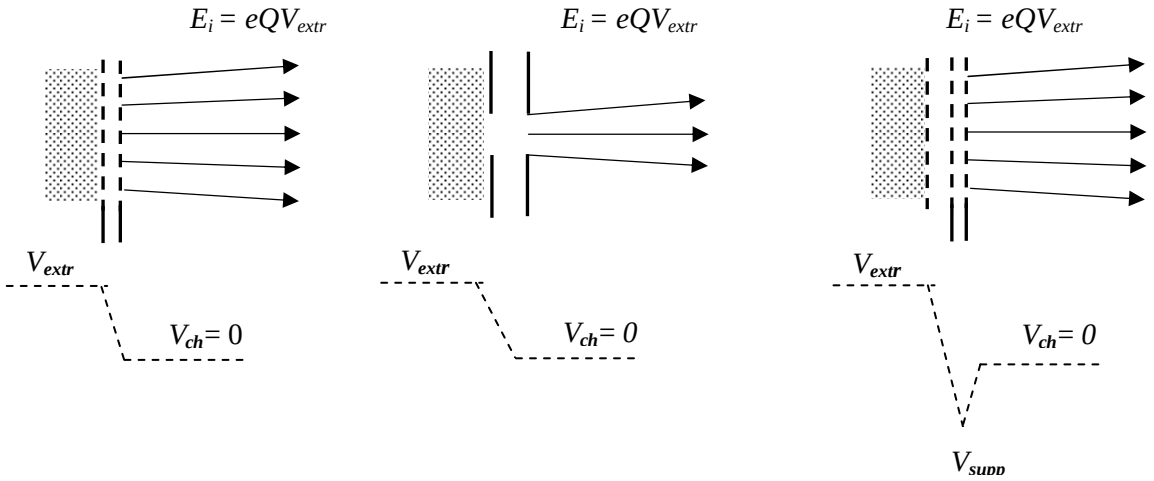

Figure 1.4. Simplified schematic of some different kinds of extractor systems.

Our more-or-less fully-developed elemental ion source can now be drawn as shown in Figure 1.5. In this setup, we use a high voltage power supply to bias the plasma to high positive voltage, and to set the extraction voltage; this power supply is often called the extractor power supply, and its voltage is the extraction voltage or the acceleration voltage.

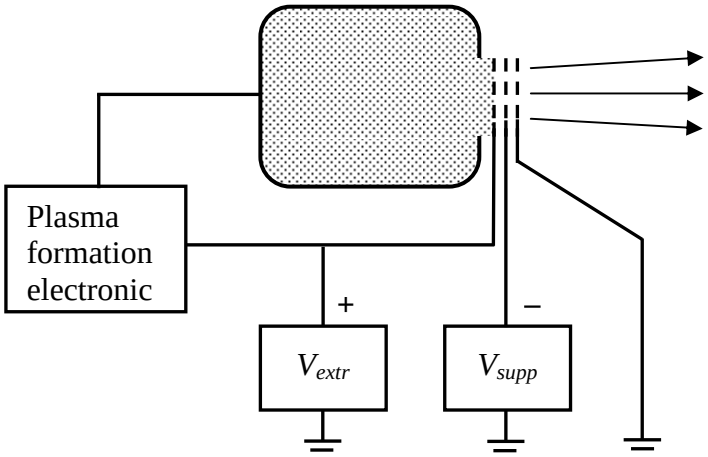

Figure 1.5. Elemental ion source showing all essential component parts

This is the voltage that determines the ion energy. Plasma formation requires its own power supplies and electronics systems, and this entire electrical package must be biased at the extraction voltage, since the plasma and plasma containment device are also at extraction voltage. This specific concern, providing the high-voltage-biased plasma electrical system, often adds considerable expense and complication to an ion source system. The ion beam formation electrode system, i.e., the extractor, that we have chosen in this example is a three-grid, multi-aperture system. The first grid (nearest the plasma), also called the plasma electrode or plasma grid, is held at extraction voltage, and might be tied directly to the plasma chamber or there might be some small degree of electrical separation between the plasma chamber and the plasma electrode. The middle grid is the suppressor electrode, and it is held at a fixed negative voltage to inhibit the backflow of electrons into the ion source; the suppressor voltage might be of the order of 10% of the extractor voltage. The third grid is the ground electrode, at the same potential (ground) as the space into which the ion beam is being injected.

1.5. Ion Beam Parameters

The ion beam formed by an ion source can be specified by many different parameters, and all of the parameters can be varied according to the ion source

design and operation. Some of the parameters are determined by the plasma source, some by the ion beam extractor, and some by the overall system geometry. There can be interaction between the various parameters, and not all are freely variable.

The ions formed can be of many different kinds. The ions might be gaseous or metallic (formed from a gas or from a metal, e.g., He^+ or Ti^+), atomic or molecular (ionized atoms or ionized molecules, e.g., N^+ or N_2^+), singly, doubly or multiply ionized (e.g., Ar^+ ,Ar^{2+} or Ar^{n+}), or as is very often the case, a mixture. These parameters are determined by the plasma source, as opposed to the extraction system or geometry or other. An important part of understanding the overall ion source is the physics of the plasma formation and plasma confinement system; ion source physics is plasma physics.

The ion beam might be operated in a *DC* mode or in a repetitively-pulsed mode. If pulsed, the pulse length might be as long as hundreds of milliseconds (longer than this might be referred to as a switched *DC* mode) or as short as nanoseconds. Beam pulsing can be achieved either by pulsing the plasma source or by gating the beam electrically (or magnetically, or even mechanically). Operating the plasma source in a repetitively pulsed mode has the advantage that the mean power levels are lower. Then the electrical systems can be smaller, and concerns such as floating of power supplies to extraction voltage and source heat removal are reduced by a factor equal to the reciprocal of the duty cycle, which can be a large factor. On the other hand, plasma rise and decay times are often of the order of microseconds to hundreds of microseconds or more, and for sub-microsecond beams it is in general necessary for the beam to be gated rather than the plasma, for example by using a pulsed extractor configuration.

The beam energy and beam current are fundamental defining parameters. The term beam energy refers to the energy per ion in the beam, and is given by *Eq*. (1.3) as the product of the ion charge and the extraction voltage. It is usual that the beam energy is stated in units of *eV* or *keV* or *MeV*, although sometimes simply voltage units are give, *V* or *kV* or *MV*; if the ion charge state is greater than unity, there is some imprecision in using voltage units. In a high vacuum ambient the ions propagate with no significant loss of energy by collisions with the background gas. But for higher vacuum system gas pressures, perhaps starting in the 10^{-4}–10^{-6} *Torr* range depending on the particular beam ions and beam setup, collisions with background gas neutrals can lead to reduced beam energy as well as other effects. The beam current is the total current carried by the ions in the beam, and this parameter too can be affected by gas pressure. Collisions with neutral atoms in the gas ambient can be charge-exchange

collisions, in which the electron of a cold atom is transferred to a fast ion, leaving a fast neutral and cold ion. For example, for the case of a hydrogen ion beam (protons), passing through a region of high neutral hydrogen gas pressure (a “charge exchange cell”, if done deliberately), the charge exchange reaction would be

$$H^{+}_{fast} + H^{0}_{slow} \rightarrow H^{0}_{fast} + H^{+}_{slow} \tag{1.4}$$

In this case a measurement of the beam current based on calorimetric measurement will include the neutral atom flux. Another complicating factor in the measurement of ion beam current is the effect of electrons – electrons formed by ion–neutral collisions in the background gas, and secondary electrons formed by ion collisions with the metal electrodes of parts of the extractor (“scrape-off electrons”) and by ion collisions with the beam target. These low energy electrons will form a background sea within which the ion beam propagates, held to the beam location by the positive space charge of the beam. The space-charge-neutralizing feature of the background electrons is a desirable feature that can be critical to beam propagation for the case of a high current beam – the ion beam maintains its integrity against “space-charge blow up” because the electrons neutralize, or compensate, the repulsive forces due to the positively charged ions. However, the cold electrons, and especially that component formed as secondaries from the ion beam target, make problematic the measurement of beam current via the current to a biased collector plate. The presence of electrons within the beam is usual, though not universal. In many cases, special effort must be taken to form an ion beam without an accompanying cold electron background.

When the ions are multiply charged the specification of ion current acquires an additional twist. Since each ion then carries a charge greater than a single electronic charge, there arise the sibling concepts of ***electrical current*** and ***particle current***. We can denote the ***electrical current*** of a beam of multiply charged ions by the symbol I_{elec} and the ***particle current*** by I_{part}. For ions of charge state $Q+$, they are related by

$$I_{elec} = QI_{par}t, \tag{1.5}$$

and thus for highly stripped ions the *electrical current* can be much greater than the *particle current*. The units *emA* and *pmA* for *electrical milliamperes* and *particle milliamperes*, and *eμA* and *pμA* for *electrical microamperes* and *particle microamperes*, have come into use to accommodate this dichotomy. Both terms are perfectly reasonable ways of describing the beam current. When the beam contains a distribution of ion charge states, the situation is yet further

complicated in that the mean charge state when expressed as the mean of the electrical current fractions can be different from he mean charge state expressed in terms of the particle current fractions.

Other beam parameters include the beam shape and size; a narrow beam or a broad beam can be formed, determined by the extractor geometry. The beam divergence and the related parameters emittance and brightness relate to the angular characteristics of the beam, and are discussed in detail in Chapters 4 and 5 and elsewhere. The ion beam energy spread is sometimes of importance; by this we refer to the spread in beam ion energy that is introduced by the thermal energy of the ions in the plasma (ion temperature) prior to extraction, by any variation in plasma potential in the pre-extraction plasma that affects the extracted ion energy, and any other energy spread effects introduced by the extractor or the downstream environment. The radial profile of the ion beam current density, $j_i(r)$, is often important, but it is difficult to form a beam whose profile is other than Gaussian for any significant axial distance from the source [5].

1.6. An Example

Here we describe an actual ion source setup as used in the laboratory and described in the literature that provides a simple example of the various design and operational features that have been outlined in the preceding sections.

The kind of source chosen for the example is a vacuum arc ion source [6, 7]. A simplified schematic of the electrical system used is shown in Figure 1.6. This system follows the approach presented in the foregoing in the following ways:

– the plasma in this case is formed by a vacuum arc discharge;

– the plasma source itself is the region labeled “Arc” in the figure.

In this particular method of plasma formation, the plasma is created at the cathode surface and streams away from the cathode toward the anode. Some of this plasma is allowed to stream away from the source through a hole in the anode toward the ion beam formation electrodes. In fact, the ion source design attempts to maximize the amount of plasma that is taken from the plasma source to the extractor.

Thus the plasma region and the extractor region are more-or-less two separate and distinguishable parts of the overall ion source configuration.

The plasma formation system is biased to high positive voltage. This includes the plasma chamber, the components that drive the arc, the triggering

system, the arc power supply, and the first grid of the beam formation electrode system (i.e., the “plasma grid” of the extractor system).

The first extractor grid (plasma grid) is tied to the anode through a resistor.

In this way the grid is held approximately at the same potential as the arc anode, while limiting the current that can be drawn to the grid (and hence limiting arcs to the grid).

The middle extractor grid (suppressor grid) is biased to a modest negative voltage. Its purpose is to stop the flow of backstreaming electrons from the downstream region back into the ion source.

The outermost extractor grid (ground grid) is tied to ground potential, which is the same potential as the grounded vacuum chamber into which the beam is transported.

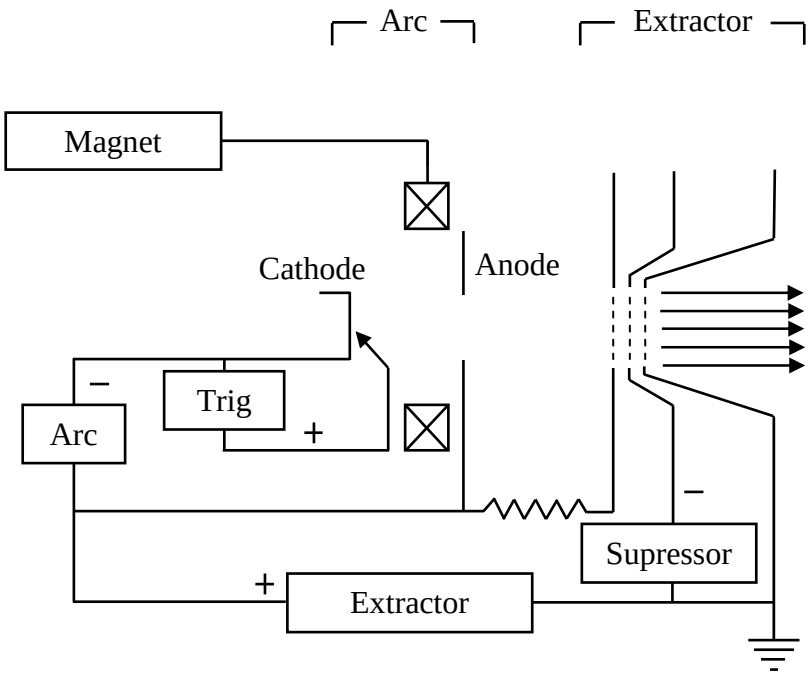

Figure 1.6. Simplified schematic of the electrical system used to drive a vacuum arc ion source

Thus we have all the components necessary to form an energetic ion beam: the plasma is formed at high voltage, and it is this voltage that determines the ion energy. Ions are created within the plasma, and they undergo a potential drop equal to the extractor voltage, between where they are created and where the beam is transported (the space external to the ion source, which is at ground potential). The suppressor grid serves its electron-blocking purpose, and its

voltage is unrelated to the ion energy. Since all of the plasma formation equipment, including the arc power supply, must be biased to extractor potential, there is some advantage in the simplicity gained by using a pulsed arc system – in this way the average power that has to be floated to high voltage is less than it would need to be for an equivalent d.c. power supply.

For this particular kind of source, the vacuum arc ion source, typical parameters could be an extractor supply voltage variable up to say 50–100 *kV*, a suppressor supply voltage that could be fixed at –1 to –5 *kV*, a pulsed arc current (current driving the arc, during the arc-on time) of say 200 *A*, an arc pulse length of say 500 *ms*, a repetition rate that could be variable in the range 1 to 50 pulses per second, and thus a duty cycle that could be variable up to several percent depending on the pulse repetition rate. The pulsed ion beam current might be several hundred milliamperes of metal ions.

Conclusion

Ion sources are widely used throughout a wide range of physics disciplines and in many related application areas. Many different kinds of sources have been developed, and the plasma physics can be complicated, but the basic underlying principles of all ion sources are simple and straightforward. Elementary ion sources can be made in the laboratory that can be perfectly adequate for many experimental purposes, and often new ideas for ion source design, construction and operation can be developed and tested in the laboratory without need for expensive and elaborate equipment. At the other extreme of the ion source spectrum, sophisticated and high performance sources with ion beam parameters pushing the limits of the possible are nevertheless still based on these elementary principles.

REFERENCES

1. Rev. Sci. Instrum. / I.G. Brown [et al.]. – 1996. – 67, 956.
2. Pierce, J.R. Theory and Design of Electron Beams / J.R. Pierce. – Van Nostrand, Toronto, 1954. – P. 177, 181.
3. Vizir, A. IEEE Trans. Plasma Sci. / A. Vizir, E.M. Oks and I.G. Brown. – 1998. – 26, 1353.
4. Forrester, A.T. Large Ion Beams / A.T. Forrester. – Wiley, New York, 1988.
5. MacGill, R.A. Rev. Sci. Instrum. / R.A. MacGill, A. Vizir and I.G. Brown. – 2000. – 71, 672.
6. Brown, I.G. Rev. Sci. Instrum. / I.G. Brown. – 1994. – 65, 3061.
7. Brown, I.G. IEEE Trans. Plasma Sci. / I.G. Brown and E.M. Oks. – 1997. – 25, 1222.

2. ION EXTRACTION

2.1. Introduction

In general an ion source consists of two parts. The first is the plasma generator that provides ion production and thus serves as an ion reservoir. The second is the extraction system for accepting ions from the reservoir and forming an ion beam. Both parts of the source may be treated independently as long as the plasma generator provides ions at the required current density and covers the whole area of the extraction system. The extraction system determines the beam properties such as ion current and beam quality in general. The extraction system thus fulfils the task of adapting the plasma generator to the beam transport system that follows.

Discussion in this chapter is restricted to the case of extraction systems with circular aperture, for extraction of positively charged ions, and without magnetic field in the vicinity of the extractor. Although extraction systems are treated in general, most examples are focused on high current, high brightness ion sources for particle accelerators.

For the case of space charge limited extraction, the Child–Langmuir law provides a fundamental means for estimating the maximum extractable ion beam current. This law is introduced together with some general aspects of extraction, followed by a theoretical description of beam quality and the emittance of an ion beam.

A refined treatment of ion extraction is then presented, considering as an example the extraction system for a high intensity proton beam designed for the IFMIF (International Fusion Materials Irradiation Facility) [1] project. Even though this treatment is given as an example, all the results are universal and can be applied to other ion species or beam energies.

Strong emphasis is placed on multi-aperture extraction systems. The effect of a multi-aperture system on the beam parameter is pointed out and exemplified by a high intensity bismuth beam (Bi^+) for the HIDIF/HIF (Heavy Ion Driven Inertial Fusion/Heavy Ion Fusion) scenario [2].

Since the initial ion energy distribution has great impact on beam formation within the extraction system, in particular on the extractable ion beam current, beam properties are discussed in terms of initial energy, thus defining the starting conditions for the extraction.

2.2. Fundamentals of Ion Beam Formation in the Extraction System

Ion extraction from a charged particle reservoir, i.e. a plasma, and ion beam formation is done by a so-called extraction system. The simplest type is a two electrode (diode) system which is shown schematically in Figure 2.1.

The extractor consists of a plasma electrode at positive potential and a ground electrode at ground potential. The electric field strength E is given by the voltage U and the distance d between plasma electrode and ground electrode. The emission surface of the ions at the plasma boundary is called the plasma meniscus [3]. Electrons coming from the plasma are reflected at this boundary if their energy is less than the potential drop between the two electrodes.

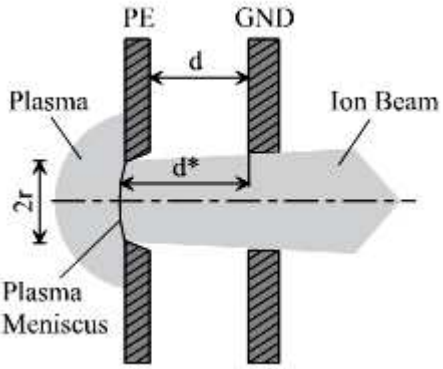

Figure 2.1. Diode extraction system and beam formation: PE – plasma electrode; GND – ground electrode; d – gap distance; d* – real gap distance; r – aperture radius

The extracted ion beam current is either limited by emission or by space-charge forces. For the second case the extractable emission current density can be calculated by the Child–Langmuir law [4, 5]. In this case the emission area is assumed to be planar and infinite, with ions having zero initial energy in the longitudinal direction (z-direction). Then

$$I_{CL} = \frac{4}{9}\pi\varepsilon_0\sqrt{\frac{2e\zeta}{m}}\frac{1}{d^2}U^{3/2} \qquad (2.1)$$

where ε_0 is the vacuum permittivity, e the electronic unit charge, ζ the ion charge state, m the ion mass, d the gap width, and U the potential drop. The electric field strength is given by $E=U/d$. Eq. (2.1) is strictly valid only for electrons coming from a fixed emitting area.

The total ion beam current that can be formed from a cylindrically-symmetric extraction system is then given by the expression

$$I_{CL} = \frac{4}{9}\pi\varepsilon_0\sqrt{\frac{2e\zeta}{m}}S^2U^{3/2} \tag{2.2}$$

where $S = r/d$ is the aspect ratio, r is the radius of the hole in the plasma electrode, and $F = pr^2$ is the emitting area.

S is constant for a given extraction system, and therefore the extractable ion beam current is proportional to $U^{3/2}$. The proportionality constant is called the perveance P of the extraction system,

$$P = \frac{4}{9}\pi\varepsilon_0\sqrt{\frac{2e\zeta}{m}}S\,. \tag{2.3}$$

The perveance P* of an ion beam is given by

$$P^* = \frac{I}{U^{3/2}}\,. \tag{2.4}$$

The current density given by Eq. (2.1) depends on the plasma density N at the plasma meniscus. All ions with a small energy component in the z-direction are able to leave the plasma. Therefore the shape of the plasma meniscus reflects the condition that the space-charge limited current density in Eq. (2.1) equals the ion current density. The distance d^* between plasma meniscus and ground electrode adjusts in such a way that the electric field strength at the plasma meniscus is zero.

Figure 2.2 shows the results of an AXCEL-INP [6] simulation for a diode system with three different plasma densities N_1, N_2, N_3. If the plasma density is too low the distance d^* increases and the emitting area is concave shaped. If the plasma density is too high (N_3) the distance d^* decreases and the emitting area is planar or even convex. Note that for all three cases the same voltage is applied. Case two is the most important case for many applications, because the ion beam trajectories have minimum divergence angles at the exit of the extraction system.

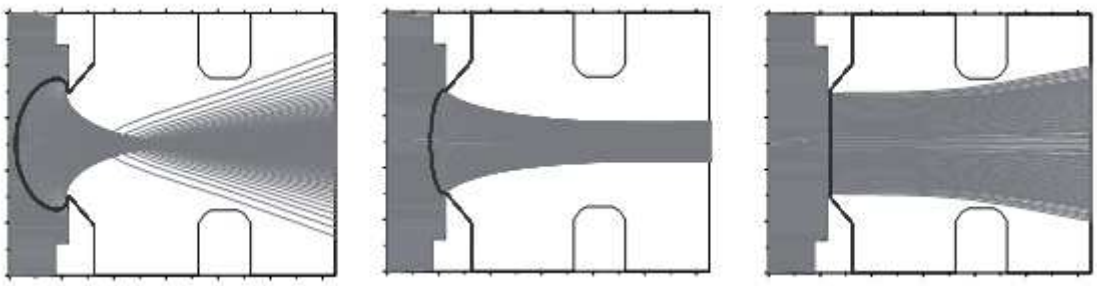

Figure 2.2. AXCEL-INP simulation for a diode system with three different plasma densities and the same voltage drop. From left to right: $N_1 < N_2 < N_3$.

For the case of a diode system, electrons that are generated within the beam channel are accelerated towards the plasma and may change the charge state distribution in the emission region. Furthermore, these electrons may not contribute to space charge compensation of the ion beam right behind the ground electrode. Without space charge compensation of the ion beam the divergence angles of the ion beam trajectories increase rapidly after extraction. Therefore a third electrode, the so-called screening or suppressor electrode, is placed between the plasma electrode and ground electrode, and held at a negative potential; we then have a three-electrode or triode extraction system. This electrode gives rise to a potential hump for these electrons. In the case of a triode system the absolute value of the negative potential has to be added to the potential used in Eq. (2.1).

Electrons generated in the ion beam have energies of a few *eV* up to a few tens of *eV*, so a potential hump of –100 *V* on the axis is high enough in most cases to screen the electrons. Figure 2.3 shows an AXCEL-INP simulation of the potential lines formed in a triode system with and without ion beam. The applied voltage is 55 *kV* for the plasma electrode and –6 *kV* for the screening electrode, the aperture radius of the screening electrode is 5 *mm*, and the length of the electrode is 4 *mm*. The minimum voltage on the axis is –1708 *V* without ion beam and –487 *V* with ion beam (see Figure 2.4).

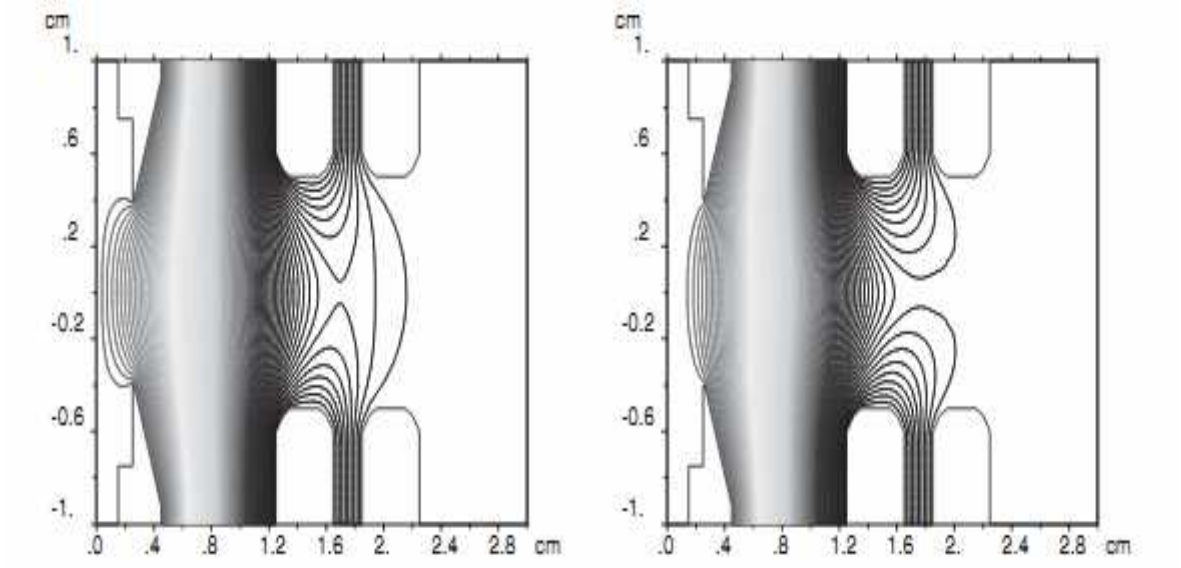

Figure 2.3. Triode system with potential lines from –6 kV to 55 kV. Electrodes from left to right: Plasma electrode (PE), screening electrode (SE), ground electrode (GND). Left: Potential lines without ion beam. Right: Potential lines with ion beam

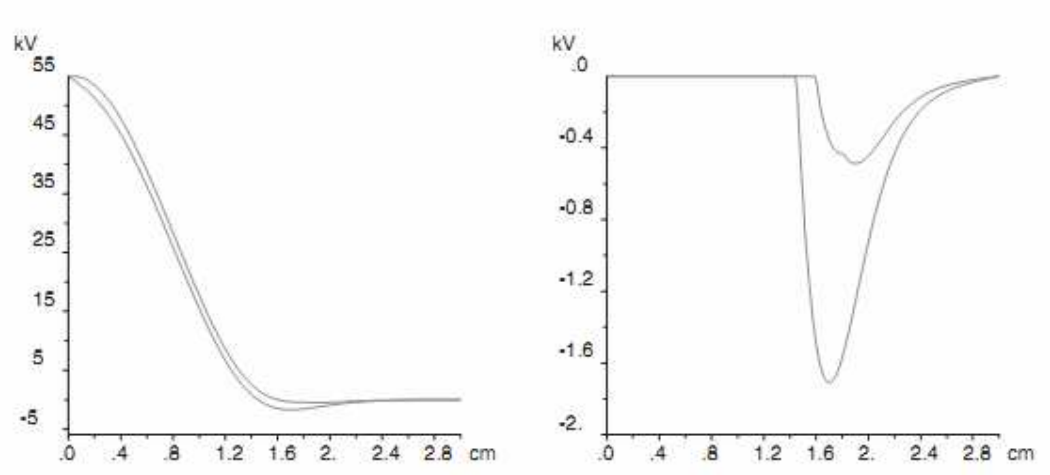

Figure 2.4. Left: Potential along the z-direction with and without ion beam. Upper curve is the potential line with ion beam. Right: Negative potential along the axis (z-direction) with and without influence of ion beam.

2.3. Beam Quality

To characterize an ensemble of particle trajectories a mathematical model of the emittance is useful. This model expresses the trajectories in terms of their position in phase space (position and momentum). The six-dimensional distribution function can be written as

$$f = f(x, y, z, p_x, p_z, t). \tag{2.5}$$

External forces as well as space-charge forces from the particles themselves are essential for the movement functions. If there is no acceleration in the z-direction, the time *t* can be replaced by position *z*. If the momentum in the z-direction is much greater than in the transverse direction (x-, y-direction), the radial momentum can be replaced by the orbital angle,

$$x' = \frac{p_x}{p_z}, \quad y' = \frac{p_y}{p_z}. \tag{2.6}$$

By superposition of single particle motion it is possible to divide the six-dimensional distribution function of Eq. (2.5) into a two- and four-dimensional subspace. We get the two-dimensional distribution functions f^*_x and f^*_y by integration of the four-dimensional Eq. (2.5) over the complementary coordinates *x*, *x*' and *y*, *y*',

$$f_x^* = \int\limits_{\neq\infty}\int f dy dy', \quad f_y^* = \int\limits_{\neq\infty}\int f dx dx'. \tag{2.7}$$

The emittance of an ion beam is the smallest area in the *2-D* subspace divided by π,

$$\varepsilon_x = \frac{1}{\pi}\iint_F dxdx', \;\; \varepsilon_y = \frac{1}{\pi}\iint_F dydy'. \tag{2.8}$$

If only conservative forces are present, Liouville's theorem is valid, stating that the density and therefore the volume in phase space is constant [7],

$$\frac{df}{dt} = 0. \tag{2.9}$$

Liouville's theorem is also valid in all subspaces of the six-dimensional phase space. This ensures that the emittance in Eq. (2.8) is a conserved value.

In accelerator physics it is common to match the emittance figure to an ellipse

$$\varepsilon = yx^2 + 2\alpha xx' + \beta x'^2 \tag{2.10}$$

with the scaling

$$\beta\gamma - \alpha^2 = 1. \tag{2.11}$$

Figure 2.5 illustrates the emittance ellipse in *x–x'* phase space.

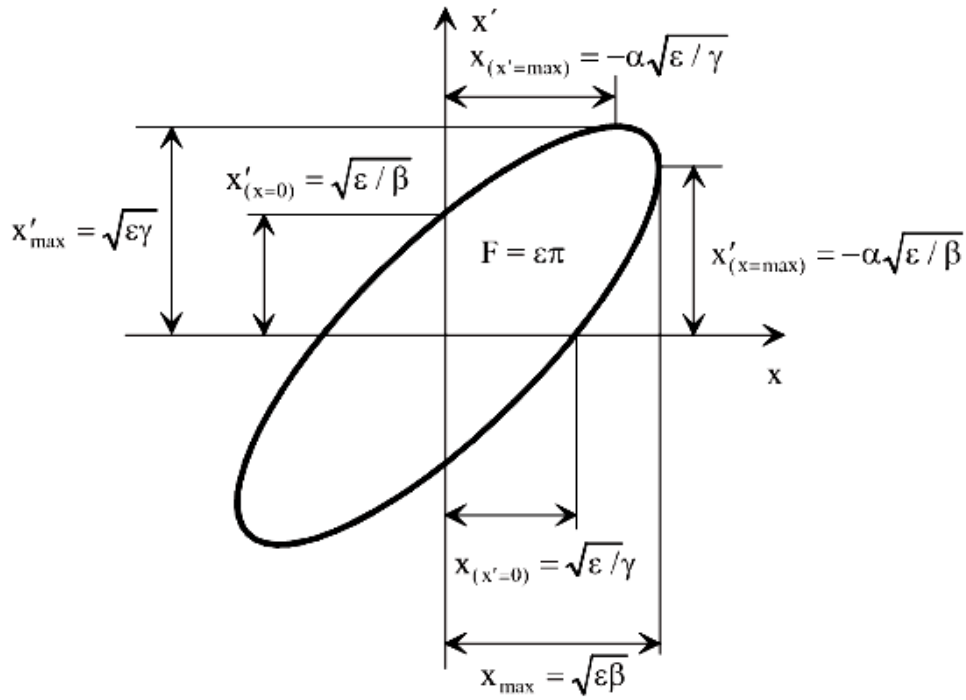

Figure 2.5. The emittance ellipse

To compare emittances at different beam energies it is necessary to normalize the emittance with the common relativistic parameters,

$$\varepsilon_{x,norm} = \tilde{\beta}\tilde{\gamma}\varepsilon_x \tag{2.12}$$

and

$$\varepsilon_{y,norm} = \tilde{\beta}\tilde{\gamma}\varepsilon_y \tag{2.13}$$

with

$$\tilde{\beta} = \frac{U}{C} \text{ and } \tilde{\gamma} = \frac{1}{\sqrt{1-\tilde{\beta}^2}} \tag{2.14}$$

where U is the speed of the ions and C the speed of light.

The relativistic parameter $\tilde{\beta}$ can be calculated from the beam parameters

$$\tilde{\beta} = 1.46 \cdot 10^{-3} \sqrt{\frac{\zeta U}{A}}, \tag{2.15}$$

where ζ is the charge state of the ion, U the acceleration voltage in *kV*, and A the ion mass in *atomic units*.

One way to compare emittances which are based on different distributions is to calculate the second order momentum from Chasman and Lapostolle. The so-called rms emittance for the two dimensional subspace is given by [8].

REFERENCES

1. IFMIF Final Report, IFMIF CDA-Team / ed. M. Martone. – Roma : Centro Ricerche Frascati, 1996.
2. The HIDIF Study, Report of the European Study Group on Heavy Ion Driven Internal Fusion for the Period 1995–1098, GSI-Report. – 1998.
3. Self, S.A. Phys. Fluids / S.A. Self. – 1762 (1963). – № 6.
4. Child, C.D. Phys. Rev. / C.D. Child. – 1911. – (Ser. 1) 32, 492.
5. Langmuir, I. Rev. Mod. Phys. / I. Langmuir and K.T. Compton. – 1931. – 3, 251.
6. Spadtke, P. INP, Junkernstrasse / P. Spadtke. – 99, 65205. – Wiesbaden, Germany.
7. Liouville, J. J. Math. / J. Liouville. – 1838. – 3, 324.
8. Sacherer, F.J. IEEE Trans. Nucl. Sci. / F.J. Sacherer. – 1971. – NS-18, 1105.
9. Guyard, J. CERN/PS/LIN 76-3 / J. Guyard and M. Weiss. – CERN, Switzerland, 1976.
10. Lapostolle, P. Proceedings of the International Conference on Ion Sources, Vienna, Austria.
11. Allison, P. Report LA-8808-MS / P. Allison, J.D. Sherman and H.V. Smith. – Los Alamos Nat. Lab., 1981.
12. Pierce, J.R. Theory and Design of Electron Beams / J.R. Pierce. – Van Nostrand, Toronto, 1954.

13. Becker, R. Rev. Sci. Instrum. / R. Becker. – 1996. – 67, 1132.
14. Rev. Sci. Instrum. / J.R. Coupland [et al.]. – 1973. – 44 , 1258.
15. Brown, I.G. The Physics And Technology of Ion Sources / I.G. Brown. – Wiley, New York, 1989.
16. Kilpatrick, W.D. Rev. Sci. Instrum. / W.D. Kilpatrick. – 1957. – 28, 824.
17. Hollinger, R. Rev. Sci. Instrum. / R. Hollinger, K. Volk and H. Klein. – 2002. – 73, 1027.
18. Rev. Sci. Instrum. / R. Hollinger [et al.]. – 2000. – 71, 836.
19. Allison, P. Comparison of Measured Emittance of an H– Ion Beam with a Simple Theory / P. Allison, J. Sherman. – CIC-14 Report Collection, LA-8808-MS, Los Alamos Scientific Laboratory. – 1981.
20. Rev. Sci. Instrum. / M. Weber [et al.]. – 1998. – 69, 1066.
21. Nucl. Instrum. Methods Phys. Res. / M. Weber [et al.]. – 1998. – A 415, 339.
22. Electron Heat Dissipation Limits on Multi Aperture Ion Source Performance : proceedings of the Second International Conference on Ion Sources / H.C. Cole [et al.]. – Wien, 1972.

3. High Current Gaseous Ion Sources

3.1. Introduction

Rapid progress in the physics and technology of high current gaseous positive ion sources was witnessed in the 1960s–1980s, driven by large-scale research projects concerned with heating of magnetically confined thermonuclear plasma [1], development of inert gas electric thrusters for space propulsion [2], and processing of materials [3]. This work resulted in the development of powerful neutral beam injectors employing quasi-steady-state sources of hydrogen and deuterium positive ion beams with current up to 100 *A* and energy up to 100 *keV*, as well as large diameter electron bombardment ion thrusters with heavy inert gas ion beams of current up to several amperes and energies of ~1 *keV* for orientation and correction of the orbit of space vehicles. With the advent of high current ion sources since the 1970s, materials technologies based on high flux ion irradiation, such as ion beam sputter etching and sputter deposition, surface modification of metals and alloys, and ion-beam-assisted deposition of coatings have seen widespread growth in both fundamental science and technological applications. The Bohm relationship for the ion current density that can be drawn from a plasma has the form [4]

$$j_i = 0,4ne(2kT_e / M_i)^{1/2}, \qquad (3.1)$$

where n is the density of the undisturbed plasma;

T_e is the electron temperature;

M_i is the ion atomic mass.

It follows that the primary means for increasing the current of ions extracted from the plasma, $I_i = j_i S$, is to increase the plasma density and/or the plasma surface area S, noting that for most plasmas Te is only weakly dependent on the discharge parameters. Note also that Eq. (3.1) implies that, all other conditions remaining equal, increase in the atomic mass of the gas leads to a decrease in the extracted ion current. For these reasons the development of high current gaseous ion sources was focused mainly on the search for efficient methods of generation of dense plasma with a large emitting surface and broad ion beam formation. A high ion current density at the plasma boundary equal to $\sim 10^2\ Acm^{-2}$ was achieved in Ardenne's source of the duoplasmatron type with geometric and magnetic constriction of the discharge column [5]. However, according to the Child–Langmuir law [6, 7] for the space-charge limited current density,

$$j_i = (4\varepsilon_0 / 9)(2e / M_i)^{1/2}(U^{3/2} / l^2) \qquad (3.2)$$

the required electric field exceeds by a large factor the breakdown field strength for such a high current density j_i. Here U and l denote the voltage applied across the accelerating gap and the gap length respectively. To increase the ion beam current Lamb and Lofgren [8] proposed reducing the density and increasing the plasma surface area using an expansion cup at the outlet of the plasma generator. However, a single-aperture beam formation system does not provide a large increase in ion beam cross-section, because the angular divergence of the ion beam grows with increasing aperture of the ion optics. To form high current beams in large area ion thrusters multi-aperture ion optics systems were first used by Kaufman [9] and then adapted for neutral beam injectors by Hamilton [10]. Efficient operation of multi-aperture ion optics requires a uniform plasma. The surface area of the plasma in high current sources may be as large as 10^3 cm^2 with a non-uniformity of ~5%. The maximum hydrogen ion beam current density, which is limited by breakdown of the accelerating gap, reaches 0.7–1.2 $A\ cm^{-2}$ at energies from 15 to 40 keV [11]. But in quasi-steady-state high current ion sources the maximum ion current density is generally restricted to $j_i \leq 0.25\ A\ cm^{-2}$ [12] due to the high power density deposited on the source surfaces and limited cooling rate. As the voltage is increased further, the limiting j_i value decreases because the working strength of the accelerating field grows quickly in accordance with Eq. (3.2). The drop in the limiting current density with decreasing voltage is due to the fact that the effective length of the accelerating gap, which depends on the electrode thickness and the hole diameter, decreases more slowly than the distance between the ion optics electrodes.

The maximum beam current density for 0.6 keV argon ions is 4.2 $mA\ cm^{-2}$ for a two-electrode system and 8.9 $mA\ cm^{-2}$ for a three-electrode system [13].

3.2. Basic Types of High Current Ion Sources

High current gaseous ion sources may be divided, according to the type of low pressure gas discharge used, into hot filament cathode sources, cold cathode sources, and high frequency plasma sources [14]. Common features of all include the use of a high current discharge and special means to provide efficient electron impact ionization of the gas, maximum utilization of plasma ions, and minimal flow of neutrals from the gas discharge system. The energy efficiency of the discharge can be defined as the ratio of the ion current at the extractor (screen or plasma) grid to the discharge power input, and is thus specified in units of $A\ kW^{-1}$.

The energy efficiency of the ion source depends on the transparency of the extraction grid and is determined by the ratio of beam current to discharge power input. Alternatively the reciprocal value – the discharge energy loss per beam ion ($eV\ ion^{-1}$) – is frequently used. Thus if the ion energy cost exceeds (as it usually does) 2–3 times the ionization energy of the gas due to additional energy loss for excitation of gas atoms, the energy cost of ions moving toward the extraction grid increases inversely proportional to the ratio of the grid area to the total ion loss area from the discharge, and the energy cost of beam ions increases inversely proportional to the transparency of the extraction grid. The energy efficiency of the ion source is a most important parameter, allowing one to estimate the degree of ion source perfection. The gas efficiency is defined by the ratio of ion current to gas flow in comparable units (ions in the beam/gas atoms into the source).

In filament driven discharges, electrons acquire their energy in the cathode sheath of the space charge and the double electric layer that is formed in the region of an abrupt change in the cross-sectional area of the discharge gap [15]. The electrons move towards the anode and dissipate their energy in plasma generation. The ion generation rate per unit volume is determined by the ratio between the density of ionizing electrons and their energy relaxation time τ_r. To improve the energy efficiency, the condition $\tau_e > \tau_r$ should be met, where τ_e is the lifetime of electrons in the plasma before impacting the anode. τ_e can be increased by a transverse magnetic field that impedes the drift of primary electrons to the anode, or an electrostatic potential distribution can be set up so that electrons oscillate within the potential well, perhaps with an axial magnetic field to help.

Most modern high current ion sources make use of multicusp magnetic field systems in which a strong transverse field is established along the periphery of the discharge system near the anode surface. The field decreases steeply with distance from the magnetic system. Such a magnetic field configuration, usually produced by rows of permanent magnets with alternating polarities, was used first by Moore [16] and then by Limpaecher and MacKenzie [17]. Primary electrons oscillate within the interior region that is virtually field-free and, because of multiple reflections of the electrons within this “magnetic bucket”, the electron distribution becomes isotropic and uniform, while the generated plasma turns out to be quiescent and homogeneous.

High frequency discharges make use of the acceleration of electrons in a high frequency electromagnetic field to energies sufficient for ionization of gas atoms. Minimizing electrode erosion is an important design feature of such sources. Whereas ECR ion sources utilize a resonance between the applied electromagnetic field frequency and the electron cyclotron frequency,

$\omega_{appl} = \omega_{ce}$ [18], dense plasmas of singly charged ions can be produced by a microwave discharge in a magnetic field that is not resonant and at higher gas pressures than for the ECR discharge. The working frequency of such microwave sources is typically 1 *GHz* to several tens of *GHz*.

Absorption of field energy can be increased, however, by choosing a field frequency of the same order as the electron–neutral collision frequency in the plasma, leading o generation of dense plasma [14]. For gas pressures typical of ion sources, this condition is met for radio frequencies (RF) in the broad range 1 to 100 *MHz*.

Cold-cathode ion sources are capable of long term operation with reactive gases. Commonly these sources employ different kinds of glow discharge plasmas with electrons oscillating in a magnetic field or a hollow cathode glow discharge with a thin wire anode [19]. However, the energy and gas efficiencies of low pressure glow discharge sources are much lower than for filament driven ion sources. This is explained by the large energy loss for the cold cathode electron emission and the relatively high gas pressure necessary for a self-sustained glow discharge. The high operating voltage of the discharge, several hundred volts, leads to ion sputtering of the cathode material and the appearance of sputtered metal ions in the beam. Such sources have a simple, robust design and are highly reliable, making them attractive for technologies non-critical to gas pressure and metal ion impurities. Gaseous ion sources using a low pressure arc with cathode spots are more efficient in energy terms [20, 21].

An interesting direction in the development of high current ion sources is the use of two-stage discharges. The first stage acts as a plasma cathode and supplies electrons to the second stage, providing conditions for efficient ionization of the gas and formation of uniform plasma. Along with the well-known duoPIGatron [22], whose first stage employs a filament type cathode, these sources include the aforementioned cathode spot arc sources. Sources with RF and microwave discharges in the first stage have been developed [23, 24], and an ion source with injection of electrons to the second stage from a hollow cathode glow discharge [25] has also been used.

Most of these sources employ a multicusp magnetic field in the anode chamber of the second stage, and they are capable of long term operation with reactive gases. In the following we consider the principles of operation, design features, and characteristics of the most common types of high current gaseous ion sources.

3.2.1. Filament Driven Ion Sources

In a duoplasmatron ion source [5] the discharge current path to the anode is through a small diameter hole (several mm) in an intermediate electrode,

ahead of which a double electrostatic space-charge layer is formed where the electrons are accelerated to an energy of several tens of electron volts. The discharge column is further constricted in the gap between the intermediate electrode and anode by a strong inhomogeneous magnetic field where a second potential jump occurs. Ionization of the gas by a dense flow of energetic electrons confined by the strong magnetic field leads to generation of dense plasma and formation of a negative anode drop in potential (~10 *V*), which prevents ions from leaving the anode. As a result an intense ion stream arises in the plasma in the direction of the outlet aperture in the anode, which is usually several millimeters in diameter. The feed gas pressure in the duoplasmatron is typically (1–2) × 10^{-2} *Torr*, the gas efficiency approaches 100%, and the energy efficiency is usually ≥ $1AkW^{-1}$.

The use of an expansion cup to reduce the plasma density and expand the surface area of the plasma not only increases the beam current but also decreases the beam emittance due to adiabatic expansion of the plasma, and decreases the level of the discharge current oscillations [26]. Duoplasmatron ion sources operating at a DC discharge current of 30 to 50 *A* and providing 1 A beams of hydrogen ions have been developed by Morgan at al. [27]. The electrodes, including the intermediate electrode, of such sources are made of copper to facilitate heat removal. A magnetic field coil wound around the anode expansion cup decreases the plasma loss and optimizes conditions for ion extraction and formation of the ion beam.

Demirkhanov [28] installed a ferromagnetic anticathode electrode to ensure oscillation of electrons in the anode region of the duoplasmatron. The anticathode was located behind a copper anode and had a potential close to the cathode potential.

Electrons oscillating in the magnetic field (1500 *G*) efficiently ionize the gas at a low pressure of ~5 × 10^{-3} *Torr*. When the anticathode negative bias relative to the anode was increased from 0 to 100 *V*, the ion current increased by a factor of five. Decreasing the gas pressure from 2 to 0.5 × 10^{-2} *Torr* increased the extracted ion current by 1.5 times. The source, which had an outlet aperture 6 mm in diameter and an expansion cup 50 *mm* in diameter, provided a pulsed hydrogen ion current of up to 1.5 *A* at a discharge current of 20 *A*.

This ion source concept, based on the use of a large scale Penning-type electrode system (PIG) to maintain a high current discharge by electrons supplied through a double electric layer from a plasma cathode, has been embodied most completely in the DuoPIGatron type ion source [29]. Figure 3.1 shows the design of a source of this kind used in a high-current, high-voltage, oxygen ion implanter [30].

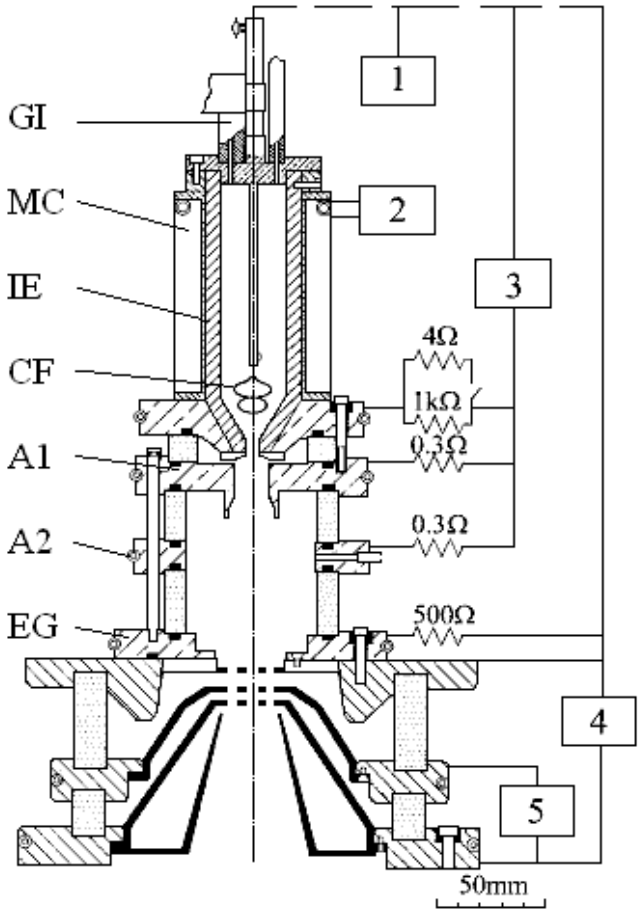

Figure 3.1. DuoPIGatron:
1 – filament power supply (65 V, 60 A); 2 – coil power supply (75 V, 1.5 A); 3 – discharge power supply (250 V, 20 A); 4 – accelerating power supply (50 kV, 0.5 A); 5 – electron suppressor power supply (2.5 kV, 20 mA); GI – gas inlet; MC – magnetic field coil; IE – intermediate electrode; CF – cathode filament; A1 – anode 1; A2 – anode 2; EG – extraction grid

The magnetic field diverges toward the ion optics, ensuring oscillation of primary electrons between the intermediate and screen electrodes and formation of a large, uniform plasma surface. To increase the cathode lifetime, an inert gas (argon) is fed into the cathode stage and oxygen into the anode stage of the source. An ion optics system with 13 holes of diameter 5 mm provided an ion beam current up to 170 *mA* at an accelerating voltage of up to 50 *kV*. After mass separation of the beam and acceleration of ions to energy of 200 *keV*, a beam of O^+ ions with current 100 *mA* was obtained. The filament cathode lifetime is over 25 hours.

The periplasmatron-type ion source [31] has a unique electrode system design, which decreases heating of the screen electrode by thermal radiation of the cathode, reduces the effect of secondary electron back flow from the accelerating gap, and ensures a high uniformity of plasma flow to the screen

grid. A rectangular variant of this source provided a hydrogen ion current of 96 *A* from an extractor 40 × 16 *cm* in size.

Another direction in the development of high-current hot-filament ion sources is the advent of single-stage, large-volume plasma generators. A magnetic-field-free source for use in neutral beam injectors has been developed in which the plasma is generated by a diffuse low-pressure high-current discharge, with a distributed thermionically emitting cathode [32]. Twenty hairpin filaments, 0.5 mm in diameter, are installed around the periphery of the discharge chamber, 14 cm in diameter, near the cylindrical wall, which serves as the anode. The peripheral placement of the cathode provides generation of uniform (–6%), oscillation-free plasma of 12 *cm* diameter. For a discharge current of 1000 *A* the deuterium ion beam current density is 0.5 A cm^{-2} and the beam current 15 *A* at an extraction voltage of 15 *kV*.

The principle of magnetic confinement of primary electrons and extraction of ions along magnetic lines using a multi-aperture extractor system was first demonstrated in the Kaufman source [13]. Figure 3.2 shows this source with an axial magnetic field, where the cathode is mounted on-axis and the cylindrical anode is located at the periphery of the chamber. The magnetic field strength, which is several tens of gauss on average, decreases in the extractor direction. The screen electrode is at floating or cathode potential. The main drawback of these systems is the radial non-uniformity of the plasma (the average-to-peak current density ratio is 0.4–0.6). For this reason, these sources use a multi-aperture extractor of diameter 10 *cm* or smaller or a single-aperture. When argon is used as a feed gas, the discharge loss is 300 to 800 $eV\ ion^{-1}$; the working gas pressure is about 5×10^{-4} *Torr*.

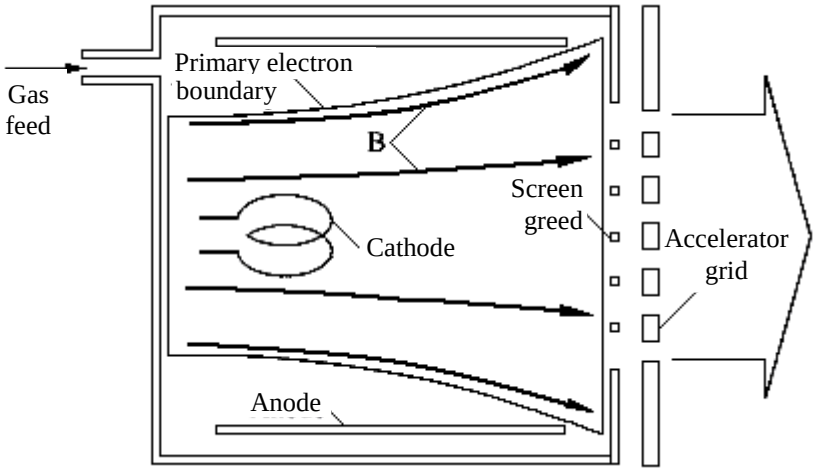

Figure 3.2. Axial field Kaufman ion source with two-grid extraction optics [13]

A considerable reduction in the ion energy cost and improvement of the mass utilization efficiency, essential for space propulsion ion thrusters, was first accomplished in Moore's source with a magneto-electrostatic containment discharge chamber [16] where a particular array of permanent magnets and multiple strip anodes was used. The anode electrodes were located in the region of strong transverse magnetic field between the magnetic poles of the multicusp structure. The decrease in the effective surface area of the anode creates a positive anode drop in potential, preventing flow of ions to the anode. An additional anode immersed in the plasma is required for stable discharge operation. Later [17] the use of a multicusp magnetic field was proposed for the formation of dense uniform plasma in large-scale systems. However, at high gas pressure, which is necessary for generation of high-density plasma, negative plasma potential relative to the anode could not be obtained throughout the entire volume of the discharge chamber. Moreover, the discharge efficiency was impaired at high gas pressure [33].

The cathode filaments in electrode systems that use a multicusp magnetic field are located in the magnetic-field-free region, and primary electrons oscillating in the plasma can move to the anode only along magnetic field lines. The electron loss area is small, and is determined by the total length of the poles and the effective thickness of the magnetic slits, which are about twice the primary electron gyroradius [34]. Low energy plasma electrons and ions are confined in the plasma by the combined action of the magnetic field and the self-consistent electric field.

A single ring-cusp magnetic field produced by permanent magnets was used in the ion source of a neutron generator (Figure 3.3) [35]. All the components of the cylindrical discharge chamber, except the cathode and the anode, are at floating potential. The shape and position of the discharge system electrodes and the parameters of the magnetic field in this source were optimized carefully. As a result a deuterium ion beam with current up to 0.2 *A* and ion energy of 200 *keV* was formed at a discharge current of 10 A and a low gas pressure of 0.25 Pa using a 1.3 cm single-aperture ion extractor.

An example of a technological ion source of this type is the CHORDIS (cold or hot reflex discharge ion source) [36], in which the end-plate electrodes of the discharge chamber are at cathode potential and the cylindrical anode is lined with 18 permanent magnets producing a multicusp field. A filament cathode (for the cold version) or a vapor generator (for the hot version) is installed opposite to the screen electrode of the ion optics. The cold version of the source has a single-aperture ion extraction system with hole area of 2 cm^2

and provides a 71 *mA* beam of xenon ions at an extraction voltage of 50 *kV* and a discharge power of 1.8 *kW*.

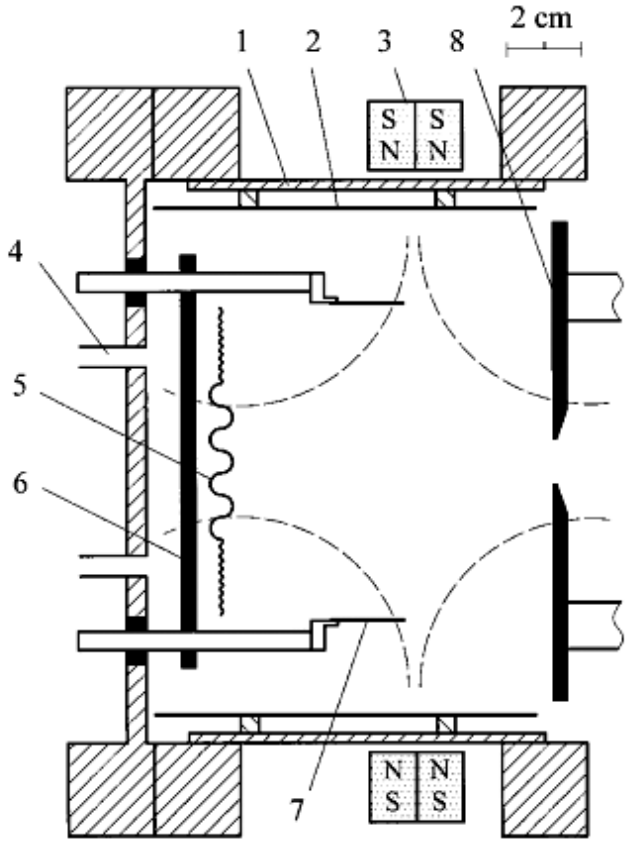

Figure 3.3. Single ring-cusp ion source [35]. Dashed lines show the shape of the magnetic field: 1 – vacuum chamber; 2 – heat shield; 3 – magnet ring; 4 – gas inlet; 5 – cathode filaments; 6 – reflector; 7 – anode ring; 8 – aperture plate

High gas efficiency (up to 90%) and low energy loss (80 $W\,A^{-1}$) have been achieved in a laboratory model of an inert gas thruster [37] in which a ring-cusp magnetic field is produced by three rows of samarium–cobalt permanent magnets mounted on the cylindrical wall of the discharge chamber 25 *cm* in diameter. A thermionic hollow cathode was placed on the axis of the chamber, while all elements of the discharge chamber, except the cathode and the screen electrode of the ion optics, were at anode potential. For a xenon pressure of $1.3–13 \times 10^{-3}$ *Pa* dense highly ionized (≥10%) plasma is generated in the chamber. A beam of xenon ions with current up to 6 *A* is formed with a multi-aperture ion optics system. About 95% of the beam is contained within a 14° half-angle.

High-current ion sources with a large number of magnetic cusps have been termed “bucket-type” ion sources. The discharge chamber of these sources, which is at anode potential, is almost fully lined with permanent magnets.

Cathodes may be installed either on the back plate opposite to the screen electrode or the side walls of the chamber. The distance between rows of opposite polarity magnets determines the size of the region in which the field drops by a factor of e ~ 2.7. The design of a source [38] developed for neutral beam injectors is shown in Figure 3.4. The cubic discharge chamber with wall 24 *cm* long was held at anode potential, while the screen grid could be at floating or cathode potential. Rows of samarium–cobalt permanent magnets were placed every 4 *cm* on the chamber walls. The magnetic field at the poles was up to 4 *kG*. Eight tungsten filaments maintained a discharge current as high as 600 *A* at a gas pressure (D_2) of 5×10^{-3} *Torr*. The ion current density at the extraction grid reached 0.4 A cm^{-2}.

The plasma non-uniformity did not exceed 4% over a 10×10 cm^2 area. The discharge efficiency was 1.63–1.75 $A\ kW^{-1}$.

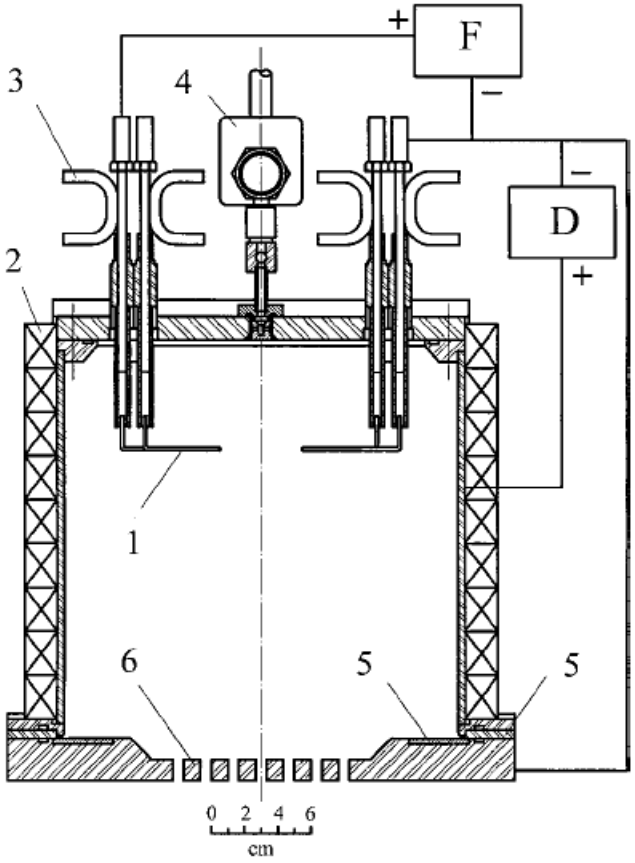

Figure 3.4. Cross-section of multicusp ion source [38]: 1 – cathode filament; 2 – SmCo magnets; 3 – cooling tube; 4 – pulsed gas valve; 5 – insulator; 6 – extraction grid; F – filament power supply (8 V, 1 kA); D – discharge power supply (80 V, 700 A)

Forrester [39] obtained higher discharge efficiency in the IBIS (intense boundary ion source) having a round chamber 25 *cm* in diameter and 40 *cm*

long. A specific feature of this source was the use of narrow iron anode strips mounted at magnetic poles, which increased the field to 0.32 *T*, and a lanthanum hexaboride hollow cathode located on the conical end face of the chamber. The plasma density uniformity is about 4% over an 18 *cm* diameter. The current density of hydrogen ions was 0.33 $A\ cm^{-2}$ at a discharge current of 330 *A* and a neutral gas pressure of 5×10^{-3} *Torr*. The overall power cost, which was estimated assuming a 30% extractor grid transparency, was less than 0.6 *kW* per extracted ampere of ion current. This high efficiency was probably due to the decreased ion loss area.

A source with a 24 × 57 cm^2 rectangular chamber 30 *cm* long, developed for neutral beam injector application, provided a hydrogen or deuterium ion current density as great as 0.4 $A\ cm^{-2}$ at the 10 × 40 cm^2 extractor grid, with a non-uniformity less than 5% [40]. The magnetic field was created by SmCo magnets arranged in 36 longitudinal rows. Thirty four tungsten filaments provided a discharge current up to 1 *kA* in a pulse 30 *s* long. The energy efficiency of the source was 0.6 A kW^{-1} at a beam current of 40 *A* and an accelerating voltage of 80 *kV*. The gas consumption was 10 to 15 mm $Hg\ l\ s^{-1}$.

A similar energy efficiency of 0.63 $A\ kW^{-1}$ was obtained in a source [41] with a rectangular chamber 25 × 40 cm^2 in size and 34 *cm* long at a hydrogen ion current density of 0.25 $A\ cm^{-2}$ at the 12 × 27 cm^2 extractor grid with 35% transparency.

Continuous linear cusps were normal to the beam axis. Six tungsten cathode filaments were mounted on the side wall of the source. When the magnetic field at the pole surface was reduced from 2.7 to 0.6 *kG* the ion source energy efficiency decreased to 0.36 $A\ kW^{-1}$.

To evaluate the suitability of this source for ion implantation and ion beam sputtering technologies, operation of the source [42] with different feed gases was studied. Ion beams of helium, nitrogen (N_2^+), oxygen (O_2^+), neon, argon, krypton and xenon were produced at currents of 23.5, 10.7, 6.2, 6.6, 6.2, 5.0 and 4.7 *A*, respectively, for an accelerating voltage of 35 to 60 *kV*, with an extractor grid with 1020 apertures each of diameter 4 mm. The discharge efficiency varied between 0.5 and 1 $A\ kW^{-1}$ at a gas pressure of 8 *mTorr*, except for oxygen (0.25 $A\ kW^{-1}$ at 9 *mTorr*).

A 38 *cm* ion source for large-capacity broad-beam etching and deposition applications generated an argon ion beam having a current of 4–5 *A* at energy of about 1 *keV* [43]. The cylindrical and end-plate parts of the discharge chamber held permanent magnets producing a multicusp magnetic field. Four hot filaments were installed on the end plate of the chamber. The required gas flow

rate was about 14 *sccm* of argon per ampere of ion beam. To obtain a high beam current at low accelerating voltage it was necessary for the extractor grids to have a large diameter-to-gap ratio. The elevated temperature at the center of the thin grids causes them to become dish-shaped. To stop the grids from touching each other, the maximum diameter-to-gap ratio was about 50. The use of "pre-dished" molybdenum grids instead of flat ones allowed a decrease in the dishing depth to about 0.1%. As a result, a diameter-to-gap ratio of nearly 400 was realized in a 38 *cm* ion source made for uniform (5% – 6%) etching of large area substrates. A 50 *cm* diameter ion source for ion beam etching and deposition is described in Ref. [44]. The source with filament-type cathodes was developed to generate beams of argon ions with energy 300–900 *eV* and current 1–5 *A*. Operation at higher current levels was possible with high-emissivity hollow cathodes.

3.2.2. High-Frequency Ion Sources

High-current RF broad beam ion sources were first developed as thrusters for space propulsion in the 1960s [45]. They have been commercially exploited for a number of industrial applications since the 1970s and used in neutral beam injectors since the 1990s. Two types of inductively coupled RF structures are most common. In one type, the induction coil is placed outside a glass or quartz cylindrical tube in which the plasma is generated. The other type has a metallic discharge chamber with an RF antenna inside the discharge plasma. According to Ref. [46], the drawbacks of ion sources with external antenna include difficulties in producing uniform plasma in large volume and rectangular shaped chambers, thermal limitations for high power RF discharge, and deposition of conducting films on the tube walls. However the beam parameters for these two types of ion sources differ insignificantly and RF ion source performance is close to that of filament driven ion sources.

The RIM-350 ion source [47], shown in Figure 3.5, employs a helical, water-cooled RF coil mounted around a quartz discharge vessel 35 *cm* in diameter. The quartz diffuser distributes injected gas around the periphery of the discharge chamber and thus improves the plasma uniformity. Due to the design of the RF coil and the RF skin-effect, high temperature electrons are distributed near the outer periphery of the discharge. Consequently the usual decrease in plasma density near the walls is compensated for, leading to a uniform distribution of current density. The ion source operates at a frequency of 1.8 *MHz*, which is in the optimal range for the source size. With an input RF power of about 2 *kW* and gas pressure of about 1 *mTorr*, the plasma is of density

5×10^{11} cm^{-3}, corresponding to an argon ion saturation current density of nearly 9 $mA\ cm^{-2}$.

The source generates beams of gas ions (Ne^+, Ar^+, Kr^+, Xe^+, O_2^+, etc.) at an ion energy in the range 50–1000 *eV* and beam current 0.15–1.5 *A*. The source is intended for various etching and deposition applications. Etch uniformity is better than 3% on targets up to 250 *mm* in diameter.

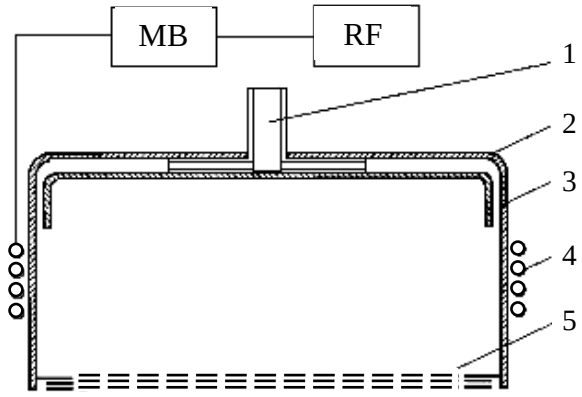

Figure 3.5. Schematic of the RIM-350 radio frequency ion source with external coil [47]: RF – RF power supply; MB – match box; 1 – gas inlet; 2 – discharge vessel; 3 – diffuser; 4 – RF coil; 5 – three-grid extraction optics

A large area RF source with external antenna [48] developed for fusion experiments used a nearly rectangular chamber with quartz walls 32 × 61 cm^2 in size and 19 *cm* long. The chamber mounted a 6 turn antenna on the outside and a water cooled Faraday shield on the inside. To improve the plasma confinement, the back-plate was covered with rows of samarium–cobalt permanent magnets. The working RF frequency was adjustable between 0.75 and 0.95 *MHz*, and the ion extraction sys-tem measured 51 × 23 cm^2.

At 120 *kW* RF power the source produced beams of hydrogen ions at 90 *A* and 55 *kV*, and deuterium ions at 75 *A* and 60 *kV*.

A 25 *cm* diameter ion source with internal antenna [46], also designed for neutral beam injection (Figure 3.6), had permanent magnets on the cylindrical wall and on the back plate of the aluminum chamber. The magnets produced an azimuthally symmetric multicusp field with magnetic field intensity at the poles of 1.5 *kG*. The diameter of the three-turn antenna of insulated copper tubing was 10–15 cm. The high frequency generator (~1 *MHz*) was rated at 30 *kW*, while the power transfer to the plasma was 90%. The RF plasma was triggered by a 50 *mA*, 45 *V* auxiliary discharge between the cathode and the chamber walls. The deuterium ion current density was 0.25 A cm^{-2} at an RF power of 20 *kW*, while

the plasma non-uniformity was 5% over a diameter of 15 *cm*. The high density and good homogeneity of the RF-generated plasma led to the development of a large RF ion source for operation with an ion extraction system of size 10 × 40 cm^2. An RF discharge in a chamber measuring 23 × 52 × 23 cm^3 with a multicusp magnetic system at the side-walls and an internal antenna shaped as a single rectangular turn 13.5 × 43 cm^2, provided an ion current density of 0.15 A cm^{-2} and 0.18 A cm^{-2} for deuterium and hydrogen ions, respectively, at a gas pressure of 4 *mm* Hg and an RF power of 25 *kW*. The non-uniformity of the ion current density was ± 7% over the extraction grid area.

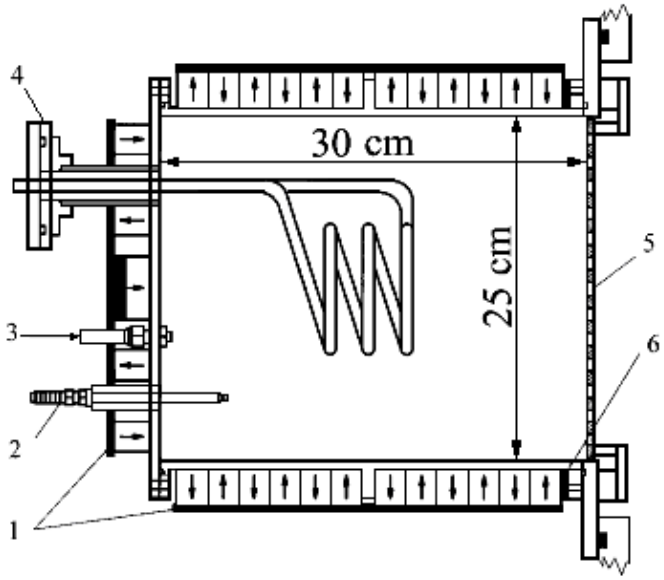

Figure 3.6. RF ion source with internal coil:
1 – pole pieces of soft steel; 2 – igniter; 3 – gas inlet; 4 – antenna feedthrough;
5 – copper end-plate with diagnostic probes; 6 – magnetic soft-steel shield

The size of the antenna coil exceeded the size of the ion extraction system to avoid damage of the antenna by backstreaming electrons from the accelerator gap. For the same reason, the permanent magnets were removed from the back-plate of the discharge chamber, since the strong magnetic fields can reflect the electron backflow toward the antenna.

A rectangular ion source [49] with a 24 cm^3 cubic copper chamber, in which Sm–Co permanent magnets produced a magnetic field with axially symmetric line cusps, and a two-turn rectangular antenna measuring 15 × 15 cm^2 was tested for voltage up to 80 *kV*. The hydrogen ion current density was as high as 0.15 $A\ cm^{-2}$.

The energy efficiency (0.6 $A\ kW^{-1}$) and the angular divergence of the beam (0.7° × 1.1°) generated by a multi-slit ion extractor proved to be no worse than for a hot-filament ion source with the same bucket chamber.

Another method for formation of large-area uniform plasmas by means of RF discharges is by using a number of small generators connected to a large volume expansion chamber, as proposed in Ref. [23]. The experiments were carried out using a single plasma generator (Figure 3.7). Dense plasma was produced in a quartz tube 3.2 cm diameter and 30 cm long equipped with an external 15 *cm* long helical antenna and a magnetic field coil to establish an axial magnetic field of up to 500 *G*. The RF radiation frequency was 14 *MHz* and the input RF power was 1 *kW*.

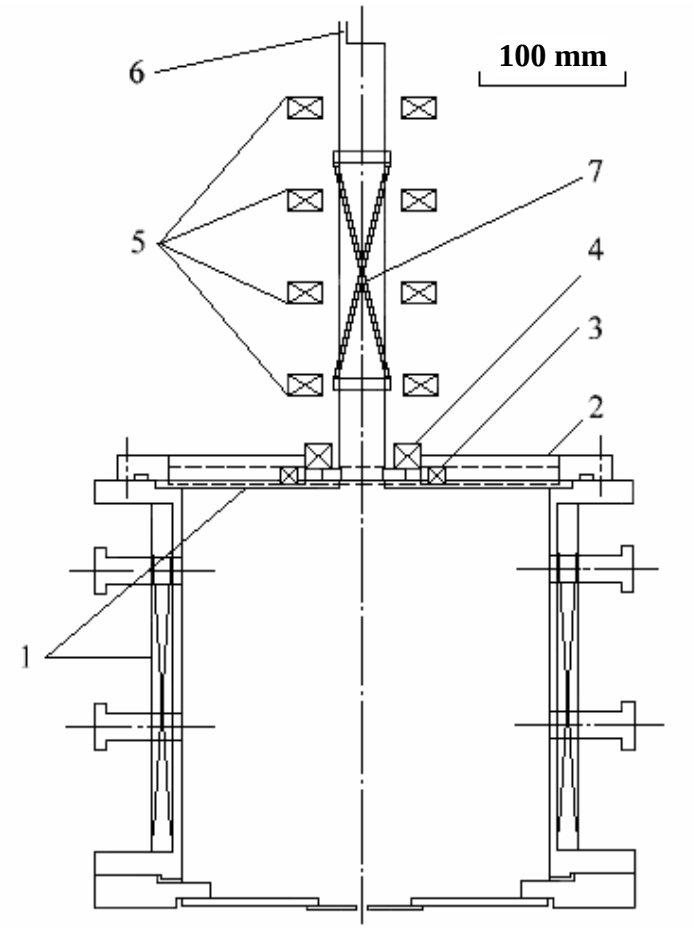

Figure 3.7. Schematic of RF plasma generator with an expansion chamber [23]:
1 – permanent magnets; 2 – end plate; 3 – ring-shaped samarium–cobalt magnet;
4,5 – magnetic coils; 6 – gas inlet; 7 – RF antenna

The 26 × 26 × 28 cm^3 expansion chamber was surrounded by 28 poles of magnetic cusp lines. The hydrogen ion current density from the plasma in the tube was greater than 80 $mA\ cm^{-2}$ for a gas pressure of 10^{-5} *Torr* and magnetic field strength of 300 *G*. The ion current density from the expansion chamber plasma increased with increasing magnetic field near the neck of the quartz tube up to values sufficient for formation of a magnetic mirror retaining the plasma in

the tube. The maximum current density obtained at a pressure of 9×10^{-6} *Torr* exhibited a linear dependence on the RF power and was equal to 2.8 $mA\ cm^{-2}$ per *kW*. The nonuniformity of ion current density distribution was –5% over the plasma region of about 14 cm^2 in size. The plasma density and uniformity may be improved if one uses more RF generators, but this complicates the design and operation of the device. Moreover, the energy efficiency of this plasma generating system is 3–4 times lower than the energy efficiency of a filament-type source with a similar chamber.

Off-resonance microwave sources [50] also provide high-current beams of singly charged ions. The discharge chamber in Sakudo's source was made as part of a coaxial wave guide separated by a vacuum-tight ceramic window. Microwave radiation (2.45 *GHz*) was fed into the chamber using a rod antenna, which served as the internal conductor of the coaxial transmission line. An inhomogeneous magnetic field with mirror ratio about 2 was produced in the discharge chamber. When the magnetic field intensity was changed over a range always satisfying the ECR condition, the absorbed power increased with increasing magnetic field, but an ECR-resonance dependence was not observed at an argon pressure of 8×10^{-3} *Torr*. Microwave energy transfer efficiency at maximum magnetic field of ~2 *kG* was over 90% and the plasma density was 10 to 100 times greater than for ECR discharges. A 40 *mm* diameter multi-aperture ion extractor was used to generate beams of argon (200 *mA*), hydrogen (400 *mA*), and oxygen (110 *mA*) ions with energy 5 *keV* for a microwave power of 600 *W*. This corresponds to an energy efficiency of ~0.67 $A\ kW^{-1}$ for the case of hydrogen ions.

An ion source in which the magnetic field satisfies the ECR condition near the plasma boundary so as to increase the extracted ion current density is described in Ref. [51]. The working frequency was 2.45 *GHz*. A specific feature of the source was that radiation was coupled into the plasma through a three-layer window. A quartz disk ensured vacuum tightness of the joint, a ceramic disk decreased microwave reflection, and a silicon nitride disk protected the window from the back-flux of energetic electrons from the accelerating gap. The ion beam was formed by a three-electrode ion-optical system with 3.5 *mm* holes having a total area of 10 mm^2. For microwave power of up to 1 *kW*, beams of oxygen, nitrogen and hydrogen ions with current up to 75 mA were generated at an accelerating voltage of up to 50 *kV*. After 700 *h* of source operation, craters up to 0.5 *mm* deep were formed on the 12 *mm* thick silicon nitride disk.

A bucket-type ion source using microwave plasma produced under ECR conditions as a plasma cathode instead of a filament cathode has been described in Ref. [24]. The ion source (Figure 3.8) employed a microwave plasma generating chamber and an arc plasma generating chamber 180 *mm* long and

200 *mm* across, surrounded by permanent magnets forming a multicusp magnetic field near the chamber wall. Electrons were extracted from the microwave plasma through a mesh grid at the sidewall of the electron-extracting electrode. When a potential difference of 30 to 70 *V* was applied between the mesh grid and the chamber walls, a plasma was formed in the second stage. The plasma discharge current increased with increasing neutral gas pressure (0.13–0.013 *Pa*) and applied voltage, and reached ~2.5 *A*. A two-grid 100 mm diameter ion extraction system with 4 *mm* diameter beamlet holes provided a pulsed (10 *ms*) 60 *mA* beam of argon ions. Another type of microwave plasma cathode was described in Ref. [52], where electrons were extracted from dense microwave-produced plasma through three holes of diameter several mm that were equally spaced one from another on a circle 60 *mm* in diameter. The main discharge chamber of diameter 200 *mm* was surrounded by 12 columns of SmCo magnets forming a line-cusp magnetic field configuration. A 115 *mm* diameter ion extractor formed high-current low-energy (1 *keV*) ion beams of 230 *mA* for argon and 132 *mA* for oxygen with excellent beam uniformity.

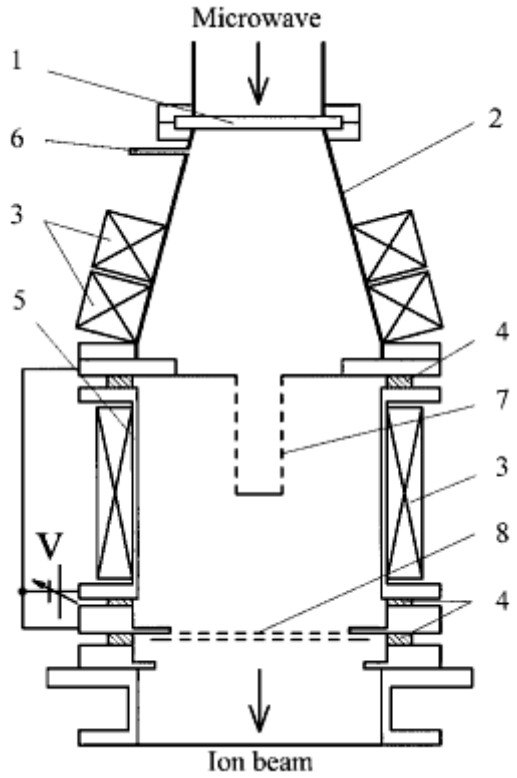

Figure 3.8. Bucket type ion source using a microwave plasma cathode:
1 – window; 2 – microwave plasma generation chamber; 3 – permanent magnet;
4 – insulator; 5 – arc plasma generation chamber; 6 – gas inlet;
7 – electron extraction electrode; 8 – ion extraction electrodes

3.2.3. Cold Cathode Ion Sources

The glow discharge can operate in a quasi-steady-state mode at a voltage of several hundred volts and current density at the cathode of up to a few tens of A cm^{-2} [53], and it is possible to use this discharge in high current ion sources. A high-current low-pressure glow discharge can be formed in hollow-cathode systems and in systems with a magnetic field to provide both radial confinement and axial oscillation ("reflexing") of ionizing primary electrons. However, large-area uniform plasmas can only be produced in weak magnetic fields. Thus the usual plasma configurations need to be modified. To ensure energy efficiency of the ion source, one needs to increase the ion current extracted from the plasma relative to the ion current to the cathode of the glow discharge. But since the ion current to the cathode determines its electron emission, effective extraction of ions changes the plasma parameters and the conditions for stable plasma operation. Some features of ion extraction and broad beam formation with glow discharge plasmas are due to the effect of the cathode sheath, whose thickness is comparable with the size of the ion optics apertures.

3.2.3.1 Basic Physics of Low Pressure Glow Discharges

For typical ranges of gas pressure p and magnetic field B used in ion sources, the voltage U_d applied across the discharge gap is localized at the cathode sheath and determines the energy of ions interacting with the cathode surface and of primary electrons supplied to the plasma. For $eU_d < 1$ *keV* the ratio between the electron and ion currents at the cathode usually does not exceed c ~ 0.1. A primary electron produces a number of ions, $N \sim eU_d/w$, provided that the full path of the electron before it goes to the anode, L, is sufficient for complete energy relaxation of the electron, i.e. the relationship $L/\lambda_i \geq eU_d/w$ is fulfilled. Here w is the energy cost of an ion in the plasma and ki is the ionization mean free path of an electron. Therefore, for self-sustained operation of the glow discharge plasma, $\gamma N = 1$, the gas pressure, which determines the oscillating electron path length L, should be high enough, and the energy required to emit an electron, eU_d/γ, is an order of magnitude larger than the energy introduced by the electron into the plasma.

According to Ref. [54], the minimum neutral gas pressure required for a hollow cathode glow discharge is determined by the ratio between the area of the outlet aperture of the cathode and the area of the cathode surface, $\eta = S_a/S_c$. For g $\sim 10^{-2}$–10^{-3} the gas pressure may be reduced to $\sim 10^{-2}$ *Pa*. However, a decrease in the anode size impedes the efflux of low energy plasma electrons to the anode in high current discharges, and consequently the discharge operating

voltage rises and the gas pressure must be increased. When $S_a/S_c < (m/M)^{1/2}$ (m and M being the electron and ion masses respectively), a space-charge double layer is formed at the outlet aperture of the hollow cathode. If the anode is placed in the cathode cavity, a positive anode drop in potential occurs.

The magnetic field that is used to confine the primary electrons also slows down the diffusion of plasma electrons to the anode. As a result the spatial non-uniformity of the plasma may increase and the plasma structure may even change. In an electrode system of the inverse magnetron type, formed by a cylindrical hollow cathode and a rod anode on the axis, increasing magnetic field leads to formation of a positive anode sheath. For low gas pressure and high discharge current, the voltage drop at the sheath may be up to several hundred volts. In a PIG electrode system with a cylindrical anode and plane end-cathodes, increasing magnetic field causes rotational instability of the plasma.

Ion bombardment leads to sputtering of the cathode material, which may consume [55] up to 10% of the energy acquired by ions in the cathode sheath, while most of the ion energy (70–90%) is released as heat. Argon ions with energy between 400 and 800 *eV*, as is typical for glow discharges, sputter 0.5–1 *atoms* ion^{-1} from an Fe cathode [56].

3.2.3.2 Glow-Discharge-Based Plasma Emission Systems

The energy efficiency of a glow discharge ion source is defined as the ratio $I_b/(I_dU_d)$ or as a/U_d, where $a = I_b/I_d$ is the efficiency of ion extraction from the discharge plasma (approximately equal to the ratio of extracted ions to the total number of ions in the plasma), U_d is the discharge operating voltage, I_b is the extracted ion beam current, and I_d is the discharge current. If the ion current is distributed uniformly over the cathode surface, a may be estimated approximately as the ratio between the surface areas of the plasma emitter and the cathode, $a \sim S_e/S_c$. However, if S_c decreases and S_e remains unchanged, the discharge operating voltage and the gas pressure need to be raised. If the primary electrons expend all their energy in the plasma, then the discharge operating voltage $U_d \sim 1/(1–a)$ [57]. Therefore, the a dependence of the energy efficiency varies as $a/(1–a)$, and the maximum of this function is $a = 0.5$. However the high gas pressure necessary to maintain the discharge at high a values limits the ion extraction and energy efficiency values of high-voltage ion sources.

Uniform plasma is generated in the hollow cathode discharge due to multiple reflections of primary electrons by the cathode sheath and collisions in the plasma, leading to an isotropic spatial distribution of electron velocities. Conversely, the use of a magnetic field in the plasma for confinement of primary electrons leads to plasma anisotropy. In an inverse magnetron plasma

configuration the anode is in the form of a thin rod on the axis of a cylindrical cathode, parallel to an applied magnetic field. Crossed electric E and magnetic B fields facilitate plasma initiation, and the low primary electron loss rate ensures a high current discharge mode at low pressure. Primary electrons emitted by the cylindrical part of the cathode drift azimuthally. The amplitude of radial oscillations of drifting electrons, which is determined by their Larmor radius $\rho = (1/B)(2mU_d/e)^{1/2}$, influences the radial profiles of the plasma density and electron temperature. Thus it is possible to control the radial distribution of the ion current density $j_i(r)$ extracted from the plasma along the magnetic field [58]. As the magnetic field increases, the distribution $j_i(r)$ with maximum current density on the axis transforms to a distribution with a minimum on the axis. The ion current density distribution is approximately uniform when ρ is approximately equal to the hollow cathode radius.

The Penning electrode system (PIG) is difficult to use in broad ion beam sources because of the substantial radial nonuniformity of the plasma. The plasma nonuniformity may be decreased if the cylindrical electrode system is fitted with a multi-component cathode. The potential difference between the ring-shaped cathode elements and the anode decreases towards the system axis. As the energy of the primary electrons drops, the ion generation rate near the axis decreases, and consequently the plasma becomes more uniform. The ion extraction efficiency in this modified PIG system is a ~ 30% because of the increased S_e/S_c ratio. The power required to maintain a glow discharge plasma may be reduced if conditions are provided for volume multiplication of ionizing electrons. Generation of primary electrons with energy eU_d as a result of ion bombardment of the cathode and acceleration of electrons in the cathode sheath requires an energy eU_d/c, where c is the ratio between the electron and ion currents at the cathode, while creation of an electron in the volume requires an average energy equal to the ion cost *w*. The ionizing capacity of the latter electron depends on the electric potential where the electron is formed. However, the rate of generation of secondary energetic electrons by ionization of the gas by oscillating primary electrons in the cathode sheath of high-current discharges in large gaps is low because of the low probability of this process, which is determined by the ratio between the sheath thickness and the size of the plasma column [59]. Two-stage electrode systems are more efficient; the low energy plasma electrons acquire additional energy in the space-charge double layer or are injected to the second stage through an artificially supported space charge layer with adjustable potential drop. Electrode systems of each stage are optimized to facilitate triggering and operation of the discharge and increase the ion current and improve plasma uniformity.

In the duoPIGatron type ion source with cold cathode (Figure 3.9) [60], ions are extracted from the plasma in the anode region of the discharge, which represents a PIG electrode system in a weak magnetic field (~10^{-2} *T*). The cathode stage with gas feed also has a smaller PIG system in a stronger (10^{-1} *T*) magnetic field. An auxiliary discharge is excited in the cathode stage at relatively low voltage and produces plasma with density sufficient to disrupt the cathode sheath in the hole between the chambers. The plasma, which penetrates to the anode region, provides conditions for initiating the main discharge. A double layer that accelerates electrons is formed near the hole. Such two-chamber systems with gas-discharge-based triggering systems were developed first for arc plasma electron sources [61] in which contribution of the plasma electrons to the electron beam current was insignificant and, therefore, a magnetic field was not used in the second stage. The main drawback of this kind of ion source is radial nonuniformity of the plasma, which can be eliminated by using a multicusp magnetic field near the anode region.

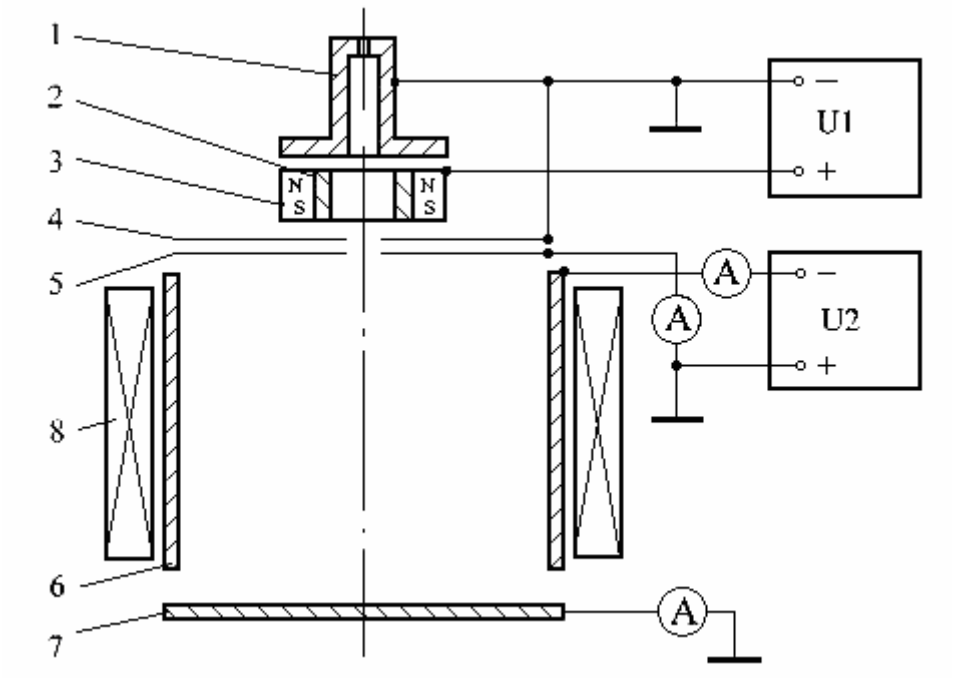

Figure 3.9. Electrode system of DuoPIGatron type ion source with cold cathode:
1 – hollow cathode; 2 – auxiliary anode; 3 – ring-shaped samarium–cobalt magnet;
4, 5 – end plates; 6 – anode; 7 – screen electrode; 8 – magnetic coil; U1 – auxiliary power supply; U2 – main power supply.

In another type of two-stage system, for example see Ref. [62], ions are extracted from the plasma generated in the cathode region, which communicates through one or several small diameter holes to a small anode chamber where the

gas feed is located (Figure 3.10). A double electrostatic layer with potential drop ~50 *V* that separates the cathode and anode plasmas appears on the cathode side of the holes.

The cathode plasma is produced by primary electrons that are accelerated in the cathode sheath and dissipate their energy by interactions with neutrals. Low energy electrons are accelerated and focused by the double layer onto the holes, where dense anode plasma is formed due to high gas density and electron flow. Plasma formation is via a beam–plasma interaction. Ions from the anode plasma are accelerated in the double layer, cross the cathode chamber, and are extracted through the screen grid holes. To facilitate discharge initiation, a PIG structure is located in the cathode region, for which purpose an auxiliary anode is installed and a magnetic field applied. The extracted ion current is distributed more uniformly for configurations with a magnetic field produced by several rows of permanent magnets fitted on the cathode [63].

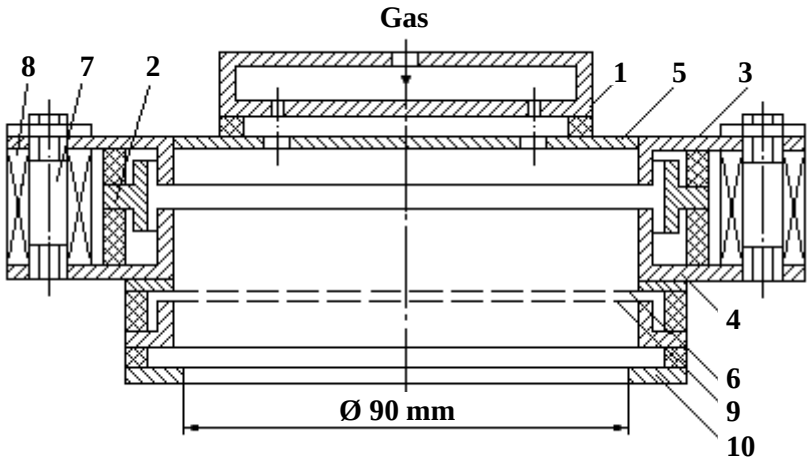

Figure 3.10. Electrode system of a technological ion source:
1 – hollow anode; 2 – auxiliary anode; 3, 4 – magnetic poles; 5 – perforated cathode disk;
6 – screen grid; 7 – magnetic core; 8 – magnetic coil; 9 – accelerating grid

A very low gas pressure (~3×10^{-5} *Torr*) was achieved in a two-stage electrode system with injection of electrons from a hollow-cathode glow-discharge plasma [25].

Electrons are injected through a fine mesh grid separating the cathode and anode regions into a chamber in which a thin-wire anode whose potential relative to the chamber walls can be adjusted independently is located. The fine grid separates the cathode and anode plasmas and ensures formation of a space-charge layer with adjustable potential drop. High transparency of the grid allows extraction of up to 90% of electrons from the first stage plasma.

Oscillation of fast electrons in the chamber housing the thin-wire anode provides efficient ionization of the gas. The efficiency of ion extraction from anode plasma in this system is determined by the ratio between the surface area of the plasma emitter and the second stage chamber walls. To increase the a value a magnetic bucket-type chamber can be used for the second stage of electrode system [64] (Figure 3.11).

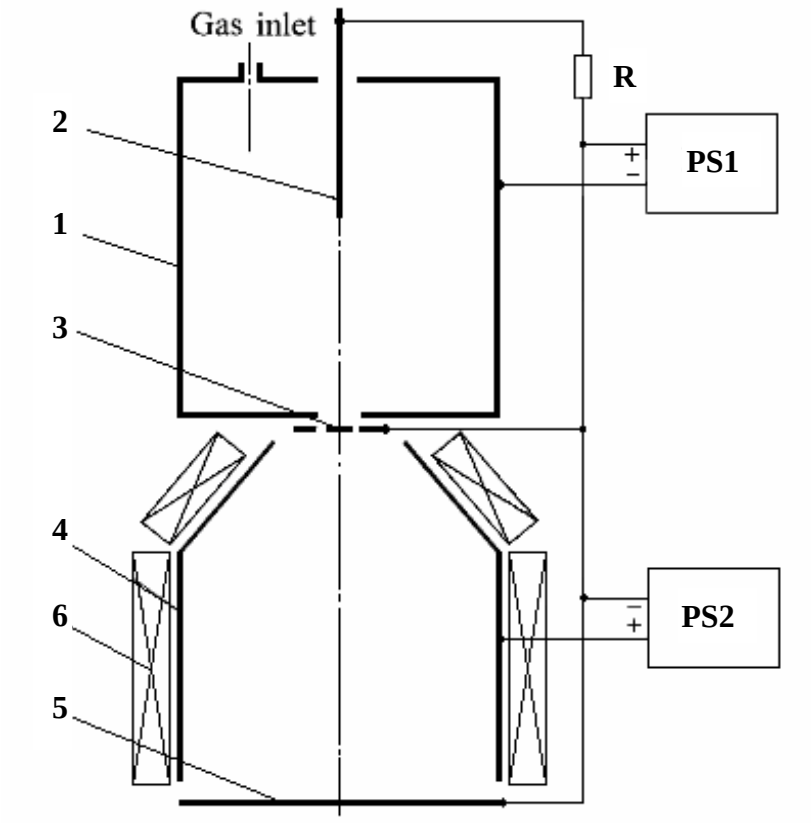

Figure 3.11. Electrode system of the bucket ion source with glow-discharge-based plasma cathode: 1 – hollow cathode; 2 – igniting electrode; 3 – fine mesh grid; 4 – anode; 5 – screen grid; 6 – permanent magnets; PS1 – glow discharge power supply; PS2 – plasma generator power supply

The power supply PS1 sustains a glow discharge between the hollow cathode and a fine mesh grid placed opposite the output aperture of the hollow cathode and connected electrically to the screen grid. Increasing the output voltage of PS2 up to ~200–300 *V* results in switching the glow discharge current (1 *A*) to the anode, while the screen grid current changes its sign and increases to values accounting for ~0.4 of the injected electron current. The ion current density distribution is close to uniform over the magnetic-field-free region of the plasma (8 cm). The rate of ion generation in the second stage depends on the

glow discharge current, the energy of injected electrons, and the gas pressure (0.01–0.05 *Pa*) which determines the ratio of the full path before going to the anode, L, to the ionization mean-free-path λ_i of injected electrons. A two-grid, 8 *cm* diameter, ion extraction system produces a 60 *mA* beam of 3 *keV* argon ions when the current of the plasma cathode is 0.2 *A*.

The mass composition and charge state of the plasma ions depend on the glow discharge current and operating voltage, and the surface conditions of the cathode. As the discharge current is increased, both the density of ionizing electrons and the flow of sputtered atoms increase. As a result, the rate of metal ion generation rises. The fractional content of metal ions in the ion beam reaches 18% for pulsed mode operation in argon with a cathode made from Al when the discharge current is 45 *A* [66]. However if the cathode temperature rises to close to thermal diffusion threshold values for the gas atoms and the feed gas reacts with the cathode material, then the content of metal impurities in the ion beam can be decreased to fractions of a percent due to the low rate of selective sputtering of metal atoms [58].

3.2.3.3 Extraction of Ions and Broad Beam Formation

There is a substantial effect of the space-charge sheath formed between the plasma and the screen grid on the position and shape of the plasma boundary and ion beam parameters; this is due to the significant potential drop and large thickness of the sheath, which is comparable with the hole diameter. In this case the location of the plasma boundary at the center of the holes depends on the field in the accelerating gap, while its position near the hole sides is determined by the sheath thickness. The effect of screen grid potential on the maximum beam current density of low energy ($\leq$ 1 *keV*) argon ions extracted from glow discharge plasma by a multiaperture three-electrode system when the electric field intensity in the beam extraction gap is close to breakdown field intensity, was studied in Ref. [66]. The dependence of ion beam current on the discharge current for the ion optics with floating screen grid was linear up to a value of saturation ion current from plasma ~10 $mA\ cm^{-2}$, while when the screen grid was at cathode potential, the rate of ion beam current increase decreased with discharge current. A computer simulation has shown that for conditions when the thickness of the cathode sheath is comparable to the radius of the ion extractor apertures, and the intensity of the accelerating field is insufficient to move dense plasma away, a convex plasma boundary is formed and the ion losses to the screen electrode increase. At lower values of plasma density and field intensity the curvature of the plasma meniscus at the extractor changes with

increasing accelerating voltage, the ion current to the extractor grid decreases, and the beam current rises. Consequently the ion extraction efficiency a may differ by 30–50% from the a value estimated from the ratio of the hole cross-section to the cathode surface area.

The parameters of the sheath between the plasma and the grid also influence the angular divergence of the beam. When the discharge voltage in a Kaufman source increases by only 18 *V*, the ion beam divergence half-angle is decreased from 12° to 9.5° [67]. The large sheath thickness in the glow discharge causes a sizeable decrease in the beam divergence; minimum beam divergence corresponds to an optimal combination of the accelerating field strength and the voltage drop in the sheath [66], if the latter is adjusted independently. In high voltage ion sources [68], (say, extraction voltage of some tens of *kV* and ion beam current density of 1–10 $mA\ cm^{-2}$), increasing the extraction gap and the hole diameter suppresses the effect of the cathode sheath and ensures both a high ion extraction efficiency and an optimal angular divergence of the ion beam. The latter, along with the ion current density distribution at the plasma boundary, influences the profile of the beam current density at the target.

3.2.3.4 Design and Performance of Cold Cathode Ion Sources

The sources described here are used primarily for ion etching of surfaces, surface modification of materials by ion implantation, and ion beam assisted thin-film deposition. Since cold cathode sources do not require power input to maintain cathode temperature, a repetitively-pulsed operational mode in which the pulse repetition rate or pulse length are adjusted can provide an efficient means for controlling the average beam current, while the optimal conditions needed for beam formation at the extractor remain unchanged. Thus materials processing can be carried out over a wide range of sample temperature and implantation dose.

Figure 3.12 shows a general view of an ion source with a plasma configuration of the inverse magnetron type [68]. The electrode system of this source consists of a stainless-steel cathode 150 *mm* in diameter and a tungsten rod anode. A magnetic field coil surrounds the source casing. A broad ion beam with circular cross-section is formed by a two-grid extractor. The total area of the 8–12 *mm* diameter beamlet holes is 70 cm^2, and the pulsed beam current for repetitively pulsed mode is 100–500 *mA* for an extraction gap aspect ratio (ratio of hole diameter to grid separation) of 0.4–0.5, and 50–100 *mA* for DC operation for an aspect ratio of 0.3–0.4. The accelerating voltage was 30 to 40 *kV*. The

discharge operating voltage was 0.5–0.7 *kV* at a current of 0.5–1 *A*, the feed gas (Ar) flow rate 30 *sccm*, and the vacuum chamber gas pressure 0.03–0.05 *Pa*.

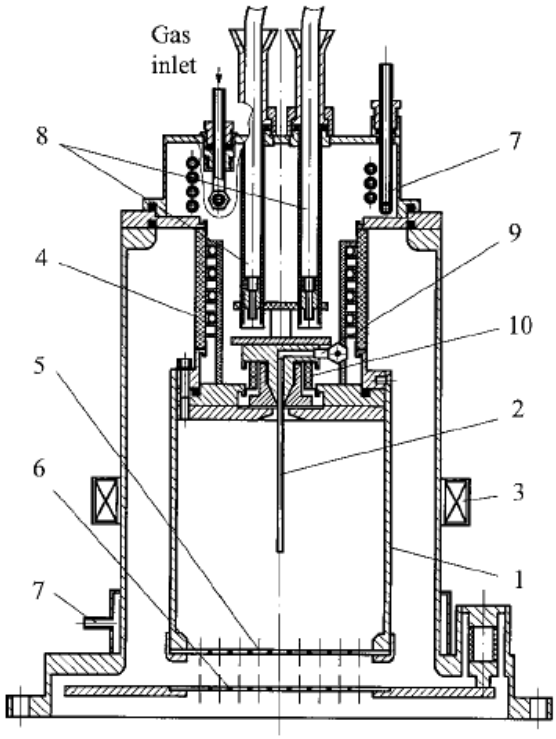

Figure 3.12. Ion source with inverse-magnetron-type electrode system: 1 – cathode; 2 – anode; 3 – magnetic field coil; 4 – high voltage insulator; 5 – screen grid; 6 – accelerating grid; 7 – water cooling jackets; 8 – cable lead-in; 9 – gas inlet; 10 – insulator

The ion beam current accounts for 5–6% of the discharge current in pulsed mode and up to 7–8% in the DC mode of beam generation. The ion extraction efficiency was increased to 16–20% by replacing the cylindrical hollow cathode by a truncated cone with base plane at the extraction grid. The value (ratio of the extracted ion current to the discharge current) decreases as the cone base angle increases. The ion current density nonuniformity is less than 10% over an area accounting for ~50% of the surface area of the cathode end face for B ~2×10^{-3} *T*. This source has been used for ion beam assisted deposition of Ti–TiN multilayer coatings to reduce the abrasive wear of blades in gas turbine engines.

Figure 3.13 shows the design of a source of low energy (~1 *keV*) oxygen ions [63]. The source includes an 18 *mm* diameter anode that is mounted on the axis of a cold hollow cathode 230 mm in diameter and 60 *mm* long. The extractor grid is fitted on the end face of the cathode. The magnetic field in the cathode chamber is produced by three circular rows of Sm–Co permanent magnets. Cathode and anode plasmas separated by a double layer with a voltage

drop of about 40 *V* are generated in this two-stage discharge. The voltage drop in the cathode sheath of the discharge is 200–300 *V*. Primary electrons that are emitted by the cathode and accelerated in the cathode sheath are confined by a magnetic field and efficiently ionize the gas in the cathode chamber. Electrons that are accelerated in the double layer lose energy through collective interactions in the anode region of the discharge. The discharge current is 0.6–1.2 *A*, and the gas flow rate 9 to 12 *sccm*. The current in the extractor circuit accounts for 40% of the discharge current and the ion beam current accounts for 13% of the discharge current. Nonuniformity of the beam current density over a 200 *mm* diameter is less than 5%. Tests for 400 *h* showed no change in the electrode geometry by ion sputtering and the source had reproducible parameters throughout the tests. The fraction of impurity metal ions in the beam of sources of this type usually does not exceed 2%.

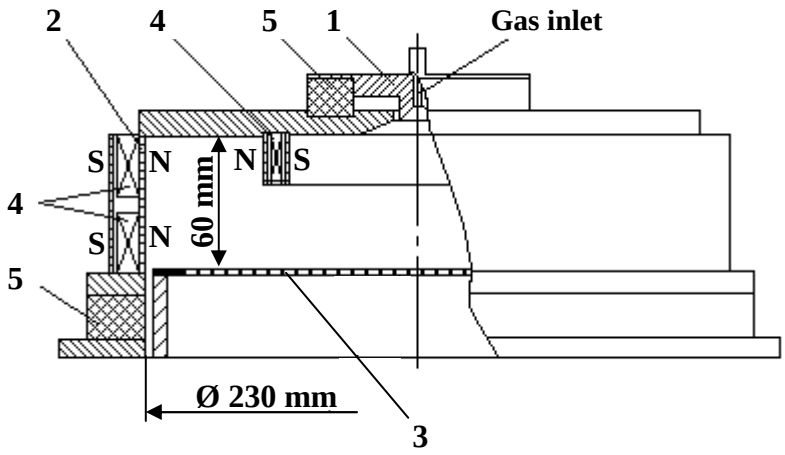

Figure 3.13. Schematic diagram of an oxygen ion source:
1 – anode; 2 – cathode; 3 – extraction grid; 4 – permanent magnets; 5 – insulator

An ion source with external injection of electrons [19] is shown in Figure 3.14. The auxiliary discharge between a hollow cathode 60 *mm* in diameter and 80 *mm* long and a fine wire mesh grid fitted in the 6 *mm* outlet aperture is initiated by dielectric flashover. Electrons are extracted through the grid and maintain the primary non-self-sustained discharge between a 12 *cm* diameter aluminum cathode and a 0.7 *mm* diameter tungsten rod anode. The injected electron current and neutral gas pressure determine the voltage across the primary gap necessary to sustain the required primary discharge current. For a primary discharge with pulsed current of 20 *A* at an argon pressure of 9×10^{-5} *Torr*, the applied voltage may be decreased from 700 to 200 *V* as the auxiliary

discharge current increases from 1 to 10 *A*. A 100 cm^2 ion beam is formed using a three-grid extractor system. The 5 *mm* diameter holes of the extractor electrode are covered with a grid of 0.5 × 0.5 mm^2 mesh size.

The beam current is up to 2 *A* in pulsed mode and up to 20 *mA* in DC mode for an extraction voltage of up to 30 *kV*. Although the fine grid expands the working range of the beam parameters for fixed extractor gap, the ion extraction efficiency decreases nearly proportionally to the grid transparency, and a (ratio of the extracted ion current to the discharge current) equals ~3.5–4%. The fraction of metal ions in the beam is less than 0.15% for a voltage across the main discharge gap of less than 100 *V*.

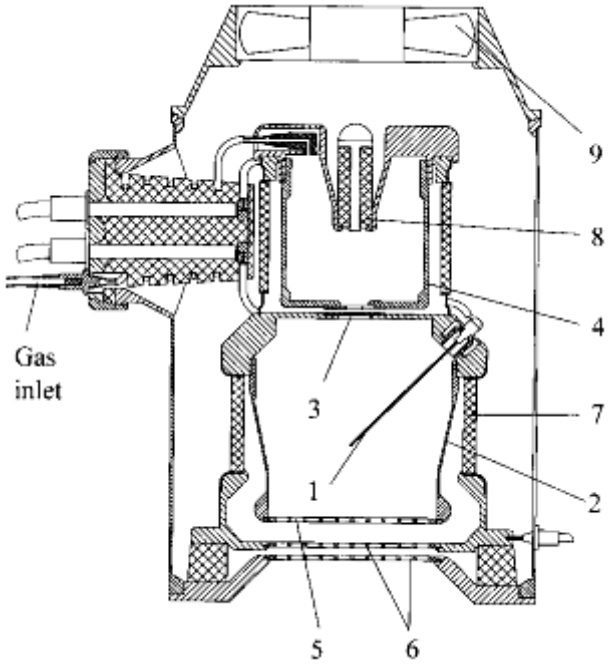

Figure 3.14 Ion source based on non-self-sustained glow discharge with injection of electrons [19]: 1 – thin wire anode; 2 – hollow cathode; 3 – fine mesh grid; 4 – hollow cathode for auxiliary discharge; 5 – screen grid; 6 – accelerating and decelerating grids; 7 – high-voltage insulator; 8 – discharge igniting system; 9 – fan for forced air cooling.

Conclusion

Dense and stable plasmas having a uniform current-density profile over large-area emission surfaces, as necessary for generation of high current beams of positive gaseous ions, can be produced using filament-driven, high-frequency and cold-cathode gas discharges. The excellent performance of available hot-filament gaseous ion sources allows generation of steady-state gaseous ion beams with unprecedented high values of beam current. The ability to generate contaminant-free, intense beams of inert or reactive gas ions has driven the rapid

development of high-frequency discharge ion sources, whose beam parameters are now not inferior to those of filament-driven sources. Recent studies of the features of low-pressure glow discharges have shown that it is possible to substantially increase the ion beam current and the energy efficiency of these sources, to decrease the metal ion content in the beam, and reduce the neutral gas pressure. We may look forward to the wide use of these kinds of ion sources in materials processing technologies. They are relatively simple to operate and maintain, and highly reliable.

REFERENCES

1. Kunkel, W.B. Fusion / W.B. Kunkel ; ed. E. Teller. – Academic Press, New York, 1981. – Chapter 12.
2. Stuhlinger, E. Ion Propulsion for Space Flight / E. Stuhlinger. – McGraw-Hill, New York, 1964.
3. Ion Implantation / G. Dearnaley [et al]. – North-Holland, Amsterdam, 1973.
4. Bohm, D. / The Characteristics of Electrical Discharges in Magnetic Fields / D. Bohm ; ed. A. Guthrie and R.K. Wakerling. – New York : McGraw-Hil, 1949. – Chapter 3.
5. Ardenne, M. Atomkernenergie / M. Ardenne. – 1956. – 1, 121.
6. Child, C.D. Phys. Rev. / C.D. Child. – 1911. – (Ser. 1) 32, 492.
7. Langmuir, I. Rev. Mod. Phys. / I. Langmuir and K.T. Compton. – 1931. – 3, 251.
8. Lamb, W.A. Rev. Sci. Instrum. / W.A. Lamb and E.J. Lofgren. – 1956. – 27, 907.
9. Kaufman, H.R. Advances in Electronics and Electron Physics / H.R. Kaufman. – New York : Academic Press, 1974. – Vol. 36. – P. 265.
10. Hamilton, G.W. Plasma Physics / G.W. Hamilton, J.L. Hilton and J.S. Luce. – 1968. – 10, 687.
11. Semashko, N.N. Ion Injectors and Plasma Accelerators / N.N. Semashko, A.A. Panasenko, and V.M. Kuligin ; ed. A.I. Morozov and N.N. Semashko. – M. : Energoatomizdat, 1990. – P. 133. – (in Russian).
12. Kunkel, W.B. Rev. Sci. Instrum. / W.B. Kunkel. – 1990. – 61, 354.
13. Sci. Technol. / H.R. Kaufman [et al]. – 1982. – 21, 725.
14. Gabovich, M.D. Physics and Technology of Plasma Ion Sources / M.D. Gabovich. – M. : Atomizdat, 1972. – (in Russian).
15. Langmuir, I. Phys. Rev. / I. Langmuir. – 1929. – 33, 954.
16. Moore, R.D. Proceedings of the AIAA 7th Electric Propulstion Conference, Williamsburg, Virginia, 1969 / R.D. Moore. – AIAA paper No.69 – 260.
17. Limpaecher, R. Rev. Sci. Instrum. / R. Limpaecher and K.R. MacKenzie. – 1973. – 44, 726.
18. Geller, R. IEEE Trans. Nucl. Sci. / R. Geller. – 1976. – 23, 904.
19. Gavrilov, N.V. Nucl. Instrum. Methods / N.V. Gavrilov and E.M. Oks. – 2000. – A 439, 31.
20. Rev. Sci. Instrum. / Yu.I. Belchenko [et al]. – 1990. –61, 378.
21. Tech. Phys. Lett. / N.V. Gavrilov [et al].– 1988. – 14, 865. – (in Russian).
22. Rev. Sci. Instrum. / R.S. Davis [et al]. – 1972. – 43, 278.
23. Oka, Y. Rev. Sci. Instrum. / Y. Oka [et al]. – 1990. – 61, 1256.
24. Nucl. Instrum. Methods / Y. Hakamata [et al]. – 1989. – B 37/38, 143.
25. Oks, E. Rev. Sci. Instrum. / E. Oks, A. Vizir and G. Yushkov. – 1998. – 69, 853.
26. Keller, R. Radiation Effects / R. Keller. – 1979. – 44, 201.
27. Morgan, O.B. Rev. Sci. Instrum. / O.B. Morgan, G.G. Kelley and R.C. Davis. – 1967. – 38, 467.
28. Demirkhanov, R.A. Tech. Phys. / R.A. Demirkhanov, U.V. Kursanov and V.M. Blagoveschenskiy. – 1964. – 34, 30. – (in Russian).
29. Rev. Sci. Instrum. / M.M. Menon [et al]. – 1985. – 56, 242.

30. Nucl. Instrum. Methods / J.P. Ruffell [et al]. – 1987. – B21, 229.
31. Fumelli, M. Nucl. Instrum. Methods / M. Fumelli and F.P.G. Valckx. – 1976. – 135, 203.
32. Vac. Sci. Technol. / K.W Ehlers [et al]. – 1973. – 10, 922.
33. Rev. Sci. Instrum. / W.L. Stirling [et al]. – 1979. – 50, 102.
34. Leung, K.N. Phys. Fluids / K.N. Leung, N. Hershkowitz and K.R. MacKenzie. – 1976. – 19, 1045.
35. Brainard, J.P. Rev. Sci. Instrum. / J.P. Brainard and J.B. O'Hagan. – 1983. – 54, 1497.
36. Keller, R.Vacuum / R. Keller, P. Spadtke and H. Emig. – 1986. – 36, 833.
37. Beattie, J.R. Rev. Sci. Instrum. / J.R. Beattie, J.N. Matossian. – 1990. – 61, 348.
38. Ehlers, K.W. Rev. Sci. Instrum. / K.W. Ehlers, K.N. Leung. – 1979. – 50, 1353.
39. Forrester, A.T. Appl. Phys. Lett. / A.T. Forrester, D.M. Goebel, J.T. Crow. – 1978. – 33, 11.
40. Rev. Sci. Instrum. / P.A. Pincosy [et al]. 1986. – 57, 2705.
41. Okumura, Y. Rev. Sci. Instrum. / Y. Okumura, H. Horiike, K. Mizuhashi. – 1984. – 55, 1.
42. Nucl. Instrum. Methods B 37/38S / M. Tanaka [et al]. – 1989. – 128.
43. Nucl. Instrum. Methods B 37/38 / H.R. Kaufman [et al]. – 1989. – 98.
44. Hayes, A.V. Rev. Sci. Instrum. / A.V. Hayes, V. Kanarov, B. Vidinsky. – 1996. – 67, 1216.
45. Loeb, H.W. Am. Inst. Aeronautics / H.W. Loeb. – 1982. – 69, 285.
46. DiVergilio, W.F.Rev. Sci. Instrum. / W.F. DiVergilio, H. Goede, V.V. Fosnight. – 1986. – 57, 1254.
47. Rev. Sci. Instrum. / V. Kanarov [et al]. – 1997. – 69, 874.
48. Rev. Sci. Instrum. / W. Kraus [et al]. – 1997. – 69, 956.
49. Rev. Sci. Instrum. / H. Goede [et al]. – 1986. – 57, 1261.
50. Sakudo, N. Nucl. Instrum. Methods B 21. / N. Sakudo. – 1987. – 168.
51. Nucl. Instrum. Methods B / G. Voronin [et al]. – 2000. – 161–163, 118.
52. Rev. Sci. Instrum. / Y. Matsubara [et al]. – 1991. – 63, 2595.
53. Abramovich, L.Yu. Tech. Phys. / L.Yu. Abramovich, B.N. Klyarfeld, Yu.N. Nastich. – 1996. – 36, 714. – (in Russian).
54. Metel, A.S. Tech. Phys. / A.S. Metel. – 1984. – 54, 241. – (in Russian).
55. Danilin, B.S. Applications of Low-Temperature Plasma for Sputtering / B.S. Danilin, V.Yu. Kireev. – M. : Energoatomizdat, 1987. – (in Russian).
56. Andersen, H.H. In Sputtering by Particle Bombardment I / H.H. Andersen, H.L. Bay, ed. by R. Behrish. – Springer-Verlag, Berlin, 1981.
57. Nikulin, S.P. Tech. Phys. / S.P. Nikulin. – 2000. – 45, 1351.
58. Sci. Technol / N.V. Gavrilov [et al]. – 1996. – A14, 1050.
59. Metel, A.S. Tech. Phys. / A.S. Metel. – 1985. – 55, 1928. – (in Russian).
60. Martens, V.Ya. Instrum. Exp. Techn / V.Ya. Martens, S.I. Bel'uk, V.N. Posokhov. – 1992. – № 2, 194. – (in Russian).
61. Kreindel Yu. E. Plasma Electron Sources / Yu. E. Kreindel. – M. : Atomizdat, 1977. – (in Russian).
62. Juravlev, B.I. Instrum. Exp. Techn. / B.I. Juravlev, V.V. Prilepskiy, V.S. Gorlatov. – 1993. – № 3, 215. – (in Russian).
63. Stognij, A.I. Instrum. Exp. Techn. / A.I. Stognij, S.V. Koryakin. – 2000. – 43, 783.
64. Gavrilov, N.V.Rev. Sci. Instrum. to be published / N.V. Gavrilov and A.S. Kamenetskikh. – 2004. – 75, 1875.
65. Визирь, А.В. Известия высших учебных заведений. Физика / А.В. Визирь, Е.М. Окс, Г.Ю. Юшков. – 2000. – 43, (№.2).
66. Gavrilov, N.V. Rev. Sci. Instrum. / N.V. Gavrilov, D.R. Emlin, S.V. Kuleshov. – 2000. – 71, 1.
67. Aston, G. AIAAJ / G. Aston, H.R. Kaufman, P.J. Wilbur. – 1978. – 16, № 5, 516.
68. Gavrilov, N.V. Russ. Phys. J. / N.V. Gavrilov, D.R. Emlin, S.P. Nikulin. – 2001. – 44, 952.

4. Application of the nitrogen ion source

4.1. Introduction

Nowadays heavy-current implantation at high densities of ion current (~1-10 mA/cm^2) has received intensive development. Numerous researches and experiments on the physical aspects of ion-beam treatment have shown that the key parameters influencing distribution of ions, phase-formation processes and, hence, level of physicomechanical properties of surfaces are density and energy of ion beam, dose of alloying and temperature. The special role is played by temperature of a warming up of samples at implantation. In case of using heavy-current ion sources irradiation process leads to appreciable warming up of surface and allows to reach temperatures providing effective diffusion redistribution of the implanted atoms. Such process of temperature implantation allows to combine advantages of traditional chemicothermal processing and ion-beam technologies. Ion-beam treatment with nitrogen for modifying high-alloy steels, such as austenitic corrosion-resistant, martensitic, ferritic and dispersion-hardening steels is especially perspective. Besides, correctly choosing parameters of ion-beam treatment make it possible to avoid formation on surface continuous fragile nitride crust.

The method of nitrogen ion-beam treatment is based on processing of materials with beams of the charged particles of nitrogen with energy ~10^3 eV and the density of current ~1–10 mA/cm^2. At an ionic irradiation at the expense of a warming up of blankets of processed details processes develop in them radiation-enhanced diffusion that provides high speed and depth of saturation of materials with nitrogen ions at rather low temperatures of processing (not exceeding 770 K). High concentration of nitrogen in surface layers of the irradiated materials, reached in the process of ion treatment, leads to radical transformations of their phase and structural condition. In particular, on the surfaces of materials processed by concentrated beams of the ions of nitrogen formation of nanodimensional amorphous layers is revealed, and in subsurface modified layers formation of new high-strength phases and fields of compressing pressure is registered. The specified structurally-phase features of the ion-modified surfaces give them high strength characteristics and resistance to wear.

So in case of nitrogen ion-beam treatment of the tool steel (C – 0,4%, Cr – 13%) level of hardness of its surface layer increases in 2–3 times, and resistance to adhesive wear increases up to 10 times.

Besides, the method of ion-beam treatment does not demand grinding and operational development operations, reduces surface roughness, does not change

the geometrical sizes of details and does not cause essential softening of subsurface layers. In particular, hardness level of tempered high-alloy tool steels after the ion-beam treatment remains at level – 50HRC. This fact supposes repeated carrying out of ion-beam treatment of the products made of such steels, without intermediate operations of thermal processings. One should admit an important advantage of nitrogen ion-beam treatment. This technology is carried out on rather inexpensive, non-polluting equipment concerns.

4.2. Experiments and tests

Presently the technology of ion-beam treatment of working surfaces of details is being mastered at the Laboratory of hardening of the Department of Technology & Equipment of Machine-building Industry of Polotsk State University. The optimum regimes and parameters of the technology for various marks of alloy steels are the main issue of the research.

For more detailed estimation of the technology we will consider process of ion-beam hardening of the cylindrical samples made from rolled sticks of industrial steel (Cr – 12%, W – 1%; Mo – 1%) (diameter – 10 *mm*, height – 6 *mm*).

The alloy steel (Cr – 12%, W – 1%; Mo – 1%) belongs to the tool semi-heatproof steels of high wear resistance. The preliminary processing of the steel (Cr – 12%, W – 1%; Mo – 1%) included heat hardening at temperature 1300 *K* (using oil) and tempering at temperature 700 – 800 *K* (during 1,5 *h*).

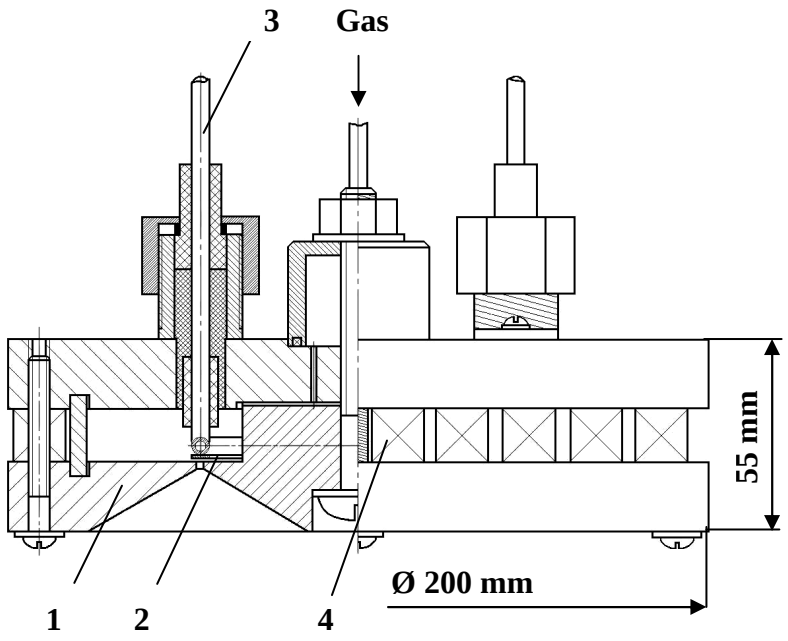

Figure 4.1. Schematic diagram of the nitrogen ion source [69]:
1 – anode; 2 – cathode; 3 – cooling water; 4 – permanent magnets

Implantation of the samples of alloy steel (Cr – 12%, W – 1%; Mo – 1%) was spent on the modernized installation UVP-70-2 within 120 minutes at energy of ions 3 *keV* and density of ion current 2 mA/cm^2 that provided fluence of alloying ~$3{,}0 \cdot 10^{19}$. Specially for the process realization has been developed the ion source, presented in figure 4.1. Temperature of the samples during the ion-beam treatment was controlled by means of the thermocouple attached to the underside of the working surface of the sample, and varied in a range 620 – 770 *K*. The beam contained ~70% of ions of the molecular nitrogen and ~30 % of ions of atomic nitrogen.

On the basis of the results of the spent experiments dependence of thickness of the modified layer on density of the ion current (fig. 4.2) has been obtained.

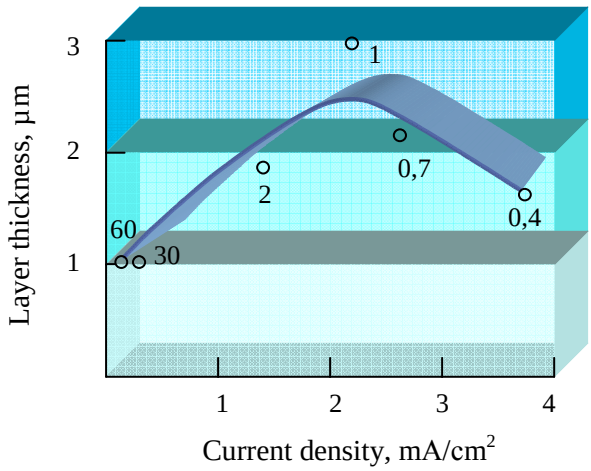

Figbre 4.2**.** Dependence of thickness of the modified layer on density of the ion current

Hardness testing of the samples was spent using the method of Vickers with hardness measuring instrument at loading 300 *N*. Microhardness of the modified layers was measured at loadings 0,19 and 0,98 *N*. Time of loading action on indenter at microhardness testing was 10 *s*, and the values mentioned in the article were defined as averages of the results of 10 measurements. The results of measurements are presented in table 4.1.

Vickers hardness (HV) testing was carried out on unimplanted surface of the samples. The obtained values characterized change of hardness of the steel in the course of high-temperature influence at ion-beam implantation. By means of measurement $H_{0,19}$ hardening degree of the implanted surface was estimated. As it is possible to see from table 2 data, at temperature 620 – 770 *K* of ion-beam treatment hardness of the steel goes down a little. Reduction of hardness of the steel at nitrogen ion-beam treatment can be connected with coagulation of carbides and relaxation of the martensite structure.

Table 4.1

Hardness HV and microhardness $H_{0,19}$ of the alloy steel (Cr – 12%, W – 1%; Mo – 1%) before and after ion-beam treatment (j ≈ 2 $mA \cdot cm^{-2}$) at various temperatures

Alloy steel (Cr – 12%, W – 1%; Mo – 1%)					
Measured parameter	Process conditions				
	Initial state	Temperature of the ion-beam treatment, *K*			
		620	670	720	770
Microhardness of the surface $H_{0,19}$, *MPa*	6100	9600-10000	16000-16500	14000-15000	10500-11000
Vickers hardness (HV), *MPa*	5950	5800	5700	5300	4900

Tribotechnical tests were spent on the laboratory tribometer, equipped with a specially developed device for measurement of the friction coefficient. The results of the measurements are presented in table 4.2.

Table 4.2

Linear wear rate I_h and friction coefficient f of alloyed steel (Cr-12%, W-1%; Mo-1%) after different regimes of treatment

Process conditions	Wear rate I_h, μm	Friction coefficient f
Heat hardening + Tempering	$1{,}47\ 10^{-2}$	0,8-0,9
Implantation with N^+ at 620 K	$1{,}49 \cdot 10^{-2}$	0,8-1,0
Implantation with N^+ at 670 K	$0{,}80 \cdot 10^{-2}$	1,0-1,2
Implantation with N^+ at 720 K	$0{,}21 \cdot 10^{-2}$	1,1-1,2
Implantation with N^+ at 770 K	$0{,}10 \cdot 10^{-2}$	0,9-1,1

Conclusion

Thus, ion-beam treatment with N^+ of the alloy steel (Cr – 12%, W – 1%; Mo – 1%) at 620 – 770 *K* with current density j = 2 $mA \cdot cm^2$ caused formation of the nitrated layers by depth from 5 – 10 micron till 30 – 35 micron with microhardness from H_μ = 9500 – 10000 *MPa* to H_μ = 14000 – 16000 *MPa*. The basic phases containing in surface layers at low temperatures of processing (620 – 670 *K*) were carbide phases Fe_3C, Cr_7C_3, nitrous martensite and ε-Fe_3N. At 720 – 770 *K* nitride phases γ' – Fe_4N and CrN formed in the surface layers. Ion-beam treatment of the steel (Cr – 12%, W – 1%; Mo – 1%) at 720 – 770 *K* led to increase in wear resistance of its blankets (in the mode of adhesive interaction) from 7 to 15 times and in friction coefficient as well.

REFERENCES

1. Derbush, S. Technology of hardening nitrogen ion-beam treatment of alloy steels / S. Derbush, N. Popok // Materials of junior researchers' conference. – Novopolotsk : PSU, 2011.
2. Ионно-лучевая обработка металлов, сплавов и керамических материалов / А.В. Белый [и др.]. – Минск : Физико-технический ин-т, 1998. – 218 с.
3. Фазовые и структурные превращения в материалах на основе железа, подвергнутых низкоэнергетической имплантации азотом при высоких плотностях тока / А.В. Белый [и др.] // ФММ. – 1995. – Т. 80. Вып. 6. – С. 82–95.
4. Wilbur, P.J. Engineering Tribological Surfaces by Ion Implantation. Surface and Coatings Technology / P.J. Wilbur, B.W. Buchholtz. – 1996. – V. 79. – P. 1–8.
5. Белый, А.В. Инженерия поверхностей конструкционных материалов концентрированными потоками ионов азота / А.В. Белый, В.А. Кукареко, А. Патеюк. – Минск : Белорус. наука, 2007. – 244 с.

LABORATORY WORK

TECHNOLOGY AND EQUIPMENT OF ION-BEAM PROCESSING OF MATERIALS

1. PURPOSE AND PROCEDURE OF EXECUTION

The aim is to study the technology of ion-beam processing of materials and equipment used, as well as the study of the influence of processing conditions on the physico-mechanical properties of the surface layers of parts.

It is recommended to carry out the work in the following order:

1. Get acquainted with the types of reinforcing materials processing.
2. To study the process and equipment for ion beam treatment.
3. Carry out training details, the sample surface.
4. To carry out the ion-beam processing of the surface of the sample in accordance with the pre-selected processing mode.
5. Carry out a quantitative assessment and comparison of microhardness of treated and untreated surfaces of samples.
6. Fill in the study protocol and report for work.

2. TYPES OF MATERIALS HARDENING TREATMENT

The increase wear resistance of machine parts subject of many investigations and research in this area is ongoing and at present [1–4].

Application forms hardening treatment is aimed at changing the physical properties of the parts in order to increase its hardness, strength, wear resistance, etc. These changes are made in all or part by volume, for example, heat treatment, or part thereof, in a so-called surface layer part by, for example, laser processing, and a protective layer (coating) of a different material [1, 2].

Currently there are many different kinds of hardening treatment, which can be divided into the following groups of signs:

1. Type of the working substance, which forms the surface layer of the part.
2. The method of generation (playback) of the working medium.
3. Type the interaction of the working substance with the surface of the component.
4. Type the working environment.

Kind of the working substance is determined by its physical state (solid, liquid, gaseous, plasma, electric field, magnetic, thermal, etc.) and the shape (solid configuration, field flow medium). Generation of the working medium is

carried out by mechanical supply and reference trajectory, heating and melting; configuration and intensity fields, ionization vapor, etc. Type of interaction of the working substance with the surface of the component is characterized by deformation (impact, static loading), chemical reactions, structural changes, diffusion or implantation of saturation, condensation and other processes. Working environment can be a vacuum, a gas (air, inert and chemically active gases), liquids, electric or magnetic fields, and combinations thereof.

Existing processes of hardening of machine parts are classified by these four groups of symptoms. These include: thermal, thermo-mechanical, chemical, thermal, chemical, electrical, electrochemical, and mechanical.

To strengthen the technological equipment and, in particular, dies and cutting tools have received the greatest application technology of the surface changes the physical properties of the parts [3]. As the working substance in these technologies use ions of refractory metals and reactive gases. The substance is generated directional electromagnetic field (beam) and implanted (implemented) in the surface of the part. Working environment is a vacuum. This treatment applies to the so-called ion-beam types of processing. Thus created on the workpiece surface or a protective coating of refractory metal compounds and gases, for example, TiC, TiN, ZrN and the like, or changing the structure and properties of the surface layer parts, for example, the introduction of nitrogen ions.

Ion-beam treatment is the process of introduction of the sample (substrate) of ionized atoms with enough energy to penetrate its surface region. The successful use of ion-beam treatment is mainly determined by the ability to predict and control electrical and mechanical properties of formed surfaces under specified conditions of implantation.

The method appeared in the early 70-ies of the last century to the field of high technologies to produce hybrid circuits, and to obtain materials with desired properties (eg, impurity semiconductors for microelectronics and alloyed with gallium arsenide for optoelectronics). The English name of the method: "The Ion-Beam Processing" or "The Ion-Beam Treatment" [4].

For a long time to bring the ion beam treatment to industrial use it was difficult. First of all, for ion beam processing equipment for all its similarity to the vacuum equipment, has a lot of aspects of how to implement a quality process of ion-beam treatment. Specialists in over thirty years of research conducted in this area, worked out modes are tailored processing technology for each particular case of the parts and tooling.

The process is carried out under high vacuum in an inert gas atmosphere (argon) in the presence of an alloying element (Fig. 1a). To cool the reaction zone and to prevent overheating of the treated material using liquid nitrogen or helium. In practice, often used cryogenic systems that achieve high vacuum and create a reliable cooling of the material being processed. At the beginning of the process provided by the vacuum of the order of ten to the minus tenth to twelfth degree mmHg. Art. Then the installation is supplied argon to a pressure of about ten to the minus of the second degree.

In case of nitriding in argon nitrogen impurity is added at the desired concentration or used target compound from a suitable nitrogen. Next, turn on the power source to maintain a high-frequency discharge. The flow of argon ions strikes the target compound from nitrogen, tearing (corroding) of its atoms and ions comprising nitrogen. Reflected from the target, the beam strikes the substrate (material being processed) implanting into the surface contained in a beam of ions and atoms of alloying element (see. Figure 1, b). In the case of nitrogen gas impurity mode adjusted to neutral atoms or argon ions bombard (etched) surface of the material being processed, creating the conditions for the penetration of nitrogen atoms and ions into the interior of the material to form a nitride gratings [5].

First of all, we should note that the crux of the ion beam processing is not in the formation of the coating, and during the introduction of any of the alloying elements and their compounds at a depth of about one micron, which forms an internal modified layer joint with the structure of the treated material and associated its crystal lattice, and in some cases this process is to form a new so-called amorphous structure, which has a positive effect on tool life.

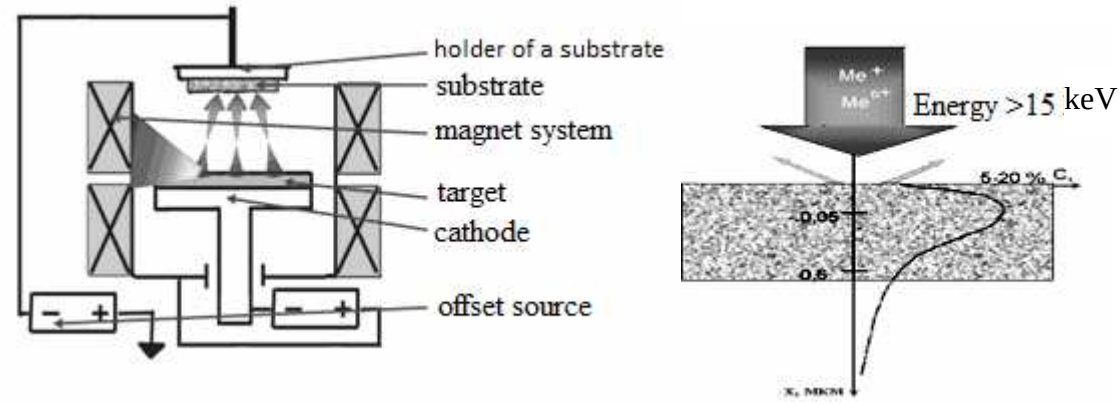

a) *b)*

Fig. 1. Schematic of *a)* the process ion beam treatment
b) and alloying element concentration distribution in the depth machined surface

When ion implantation depends on the fluence (flux integrated density) of ions can be formed in the surface layers of diluted, supersaturated (metastable) solid solutions, precipitates of new phases, as well as loss of long-range order in the arrangement of atoms forming the solid state crystal lattice. Diagram of phase states of metallic materials subjected to ion-beam treatment, is shown in figure 2.

Identification of specific concentration and temperature parameters of the implementation of a structure is a rather complicated task that requires taking into account the parameters of the ion-beam treatment (energy, angle of incidence, the charge state of the implanted particles, the ion current density, process temperature) and the initial microstructure of the processed material.

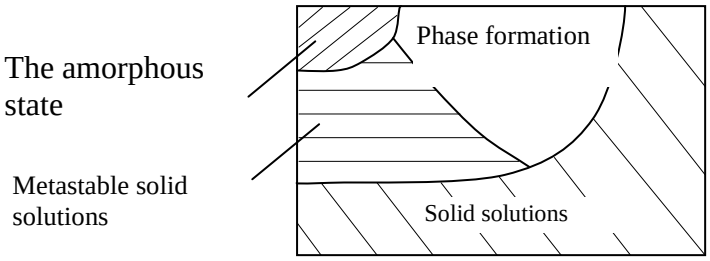

Fig. 2. Schematic illustration of phase states in metallic materials subjected to ion beam treatment as a function of the dopant concentration C and the implantation temperature Tm

Recently, ion-beam treatment, as a method for modifying the surface attracting more and more attention of specialists in various fields. This is due to [6]:

– changes in material structure and to a certain depth in the formation of the surface layer and the microhardness increased residual compression stress without changing the geometrical parameters of the surface;

– the formation of the surface layer by treatment with active ions (nitrogen, carbon, etc.) Stable chemical compounds (nitrides, carbides) which substantially alter both mechanical and physico-chemical properties of the surface;

– introducing into the surface of not only the ions of different atoms and chemical compounds, such as the creation of a solid lubricant and simultaneously hardening phase of borides, nitrides or carbides of Ti, Al, Zr, Nb.

Main advantages of ion beam treatment in comparison with other methods of doping of the surface as follows [7, 8]:

– the possibility of virtually any combination of "matrix – alloying component";

– the lack of adhesion problems, characteristic for technological coating processes;

– the size of the immutability of the workpiece holding process at all temperatures, including room and negative;

– the introduction of strict dosage amounts of dopants; exceptional purity of the process;

– the possibility of occurrence of any impurity profiles in depth;

– high reproducibility of the structures obtained; ease of management and the ability to ion beam treatment of certain parts of the surface.

3. THE PROCESS AND EQUIPMENT

The technological process of ion-beam processing of materials comprises the following steps [7]:

– Acquisition. On the operator manning the desk is made of parts to be treated the same size;

– Cleaning. The surface of the parts rubbed white calico soaked in Nefras to remove contaminants;

– Rubbing. On the surface of the component residues Nefras removed: first the white calico soaked in alcohol, and then dry calico;

– Control. To inspect the surface of the lack of grease, lint cloth. Prepared for ion beam processing items must bear silica gel up to 12 hours;

– Loading. Details are set to snap in a vacuum chamber installation PVM-0.5F. the air is evacuated from the chamber. Included rotary drive;

– Ion-beam treatment:

1. Produced ionic surface cleaning components. Time – 60–80 minutes.

2. Held ion beam processing components. Current 90A; 170 – 200^{o}C temperature; vacuum of $5 \cdot 10^{-3}$ MPa; nitrogen pressure of 0.097 Pa, 100 Pa propane; coating time of 20 – 30 minutes; BT10 titanium cathode.

3. Turns off the voltage on the ion source.

4. Stops the nitrogen supply to the camera.

5. Held filling the chamber with air, cooling and removing the snap of the camera, and parts of the rigging, cooling of 30 – 40 minutes;

– Control.

1. Visual inspection of each part (hardened surface should have a uniform color) is performed at the operator desk.

2. Controlled by micro-hardness on the sample-witness.

– Transport. Finished parts are sent to the warehouse.

Prior to the ion implantation part must undergo pre-deployment training.

The accumulated experience in the preparation of the surfaces of parts allows us to recommend the following basic steps:

– mechanical purification of the major layers of lubricant or preservative as well as cleaning in an ultrasonic bath and a specially prepared solution;

– washing in hot water;

– washing with running water and ethyl alcohol.

If necessary, enter additional rust removal operation. The item is placed in a container with a solution to remove rust, which after repeated washing operations listed. Then the item is dried in an oven. Considering the variety of items, some of their species in the technology of preparation and cleaning of surfaces subject to refinements and additions that do not cancel the above process steps.

General view of the installation PVM-0.5F for ion beam treatment of nitrogen is given in Fig. 3.

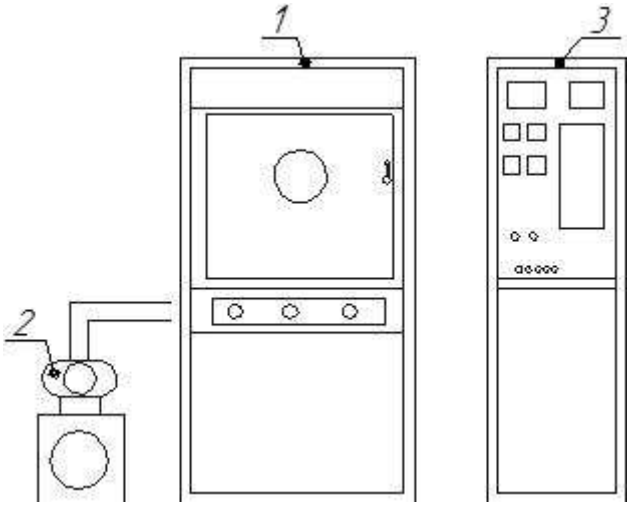

Fig. 3. General view of the installation PVM-0.5FN:
1 – the pumping monoblock post; 2 – vacuum pump ATS 50; 3 – front control

Operation on the installation presented in on its operating instructions issued to students when performing laboratory work.

4. METHOD OF RESEARCH QUALITY AND STRENGTHENING MICROHARDNESS MATERIAL

Investigation of the process of ion-beam processing and properties of the modified materials in a large number of materials, such as [8–18]. They set out the methodology and findings.

Determination of the quality of parts due to hardening of ion implantation is reduced to a visual assessment of the state of the treated surface and comparison with a standard. It should have a uniform structure and even color (without stains).

Test method Microhardness (GOST 9450) is designed to evaluate the hardness of microscopically small amounts of material. It is used to measure the hardness of individual structural components, a very thin surface layers, coatings, foils, thin wire, small parts, and so on. N.

Microhardness indentation measured standard tip under the influence of small loads from 0.05 to 4.9 N. Four types of diamond tip is used for measurement of micro-hardness: four-sided pyramid with a square base (index "square"), three-sided pyramid with a base in the form of a triangle equiaxed (index "tr"), four-sided pyramid with a rhombic base (code "RB"), bicylindrical tip ("p" index). The most widely used form of diamond tip into four-sided pyramid with a square base with an apex angle of 136°.

A device for measuring the microhardness – Micro Durometer PMT-3, developed by M.M. Khrushchov and E.S. Berkovich, shown in figure 4 *a)*. It is a microscope equipped with a special subject table and the loading mechanism, which is fixed diamond tips.

The test specimen is mounted on a microscope table device under a microscope lens. Moving the table in two mutually perpendicular directions, choose a place on the sample for measurement of micro-hardness. Then slowly turn the table with the handle lock to lock, with a selected portion of the sample is set at the tip - diamond pyramid. Then slowly (during 10 – 15) is lowered with the rod diamond pyramid so that the diamond specimen touched. After exposure 5 – 10 with the sample under load lift shaft with a tip in a starting position. Turn the table return a sample under a microscope lens and is measured with a micrometer eyepiece length of the diagonal of the impression (fig. 4 *b)*). The countdown tenths of a millimeter is carried by the figures visible in the field of view, and hundredths of a millimeter and thousandth – on a drum micrometer eyepiece, the price of which is equal to 0.3 mm division. Turning eyepiece 90°, determined by the length of the other diagonal and calculating the arithmetic mean of the lengths of both diagonals.

To determine the microhardness of the diagonal length (mm) special tables for different loads.

Microhardness numbers have the same dimension as the number of Vickers hardness or Brinell hardness: Mpa. According to number of guests Microhardness, MPa, recorded without dimension, for example, Hkv = 1810.

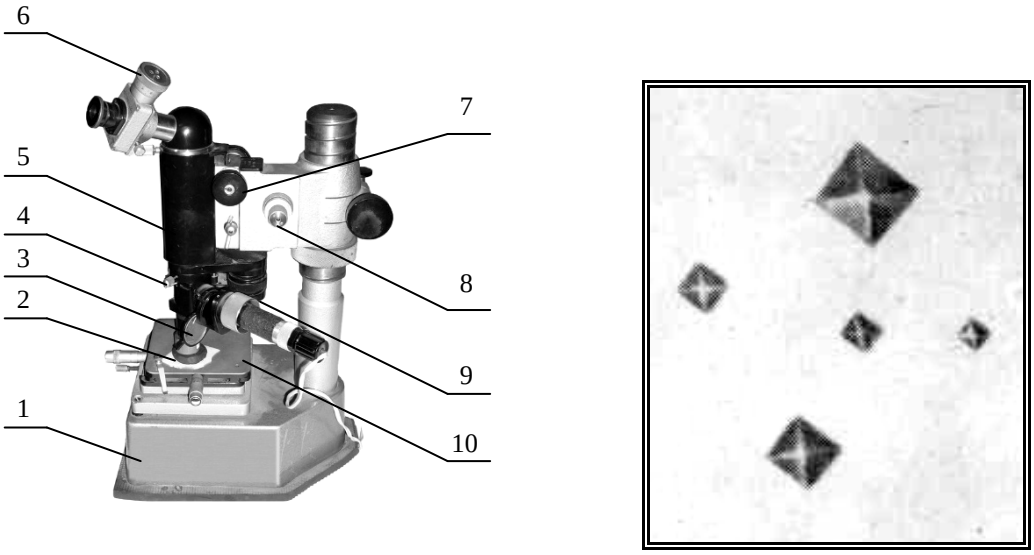

a) *b)*

Figure 4. PMT-3 microhardness tests (a) and prints microsection (b): 1 – base; 2 – sample; 3 – illuminator; 4 – screw alignment; 5 – tube; 6 – micrometer eyepiece; 7 – macrometric screw; 8 – micrometer screw; 9 – cargo; 10 – table

The surface of the sample for measurement of micro-hardness is prepared very carefully – it is ground and polished. Electrolytic polishing is recommended to avoid hardening in a thin surface layer. If necessary etched surface of the sample subjected by the same reagents which are used for microanalysis appropriate metal or alloy.

As a result of ion-beam treatment the hardness of the surface layer parts should be increased by at least 1.5 times.

Study corrosion resistance based the devastation coating by oxidative solution. Before researching the samples with a covering and without it coated on analytical balance. When tested with samples of uncoated and coated solution of hydrochloric acid (30 g / dm^3) and maintained throughout the (20 + –1) minutes at a temperature of 60 – 70 degrees. The samples weigh on the scales, the weight loss is compared and judged on their wear resistance and corrosion.

5. TASK

5.1. For a given sample of material options to choose modes of ion beam treatment.

5.2. Make ion beam processing of the sample.

5.3. Measure microhardness of the sample after processing, and compare it with the micro-hardness of the sample not subjected to the process.

5.4. Fill in the protocol process of ion-beam treatment of the sample surface and draw the necessary conclusions.

6. STRUCTURE OF THE REPORT

6.1. The name, purpose and performance of laboratory work.
6.2. Brief information on current uses and methods of hardening of surfaces of parts, process equipment and tooling.
6.3. Essence and features of ion-beam treatment, the equipment used, process conditions.
6.4. Bring protocol assigned material processing modes and measurement microhardness surfaces results (table 1–3).
6.5. Conclusions.

Table 1

Options for job

№ options for	Sample material
1	Р6М5
2	12Х18Н10Т
3	12ХМ
4	12Х1МФ
5	12ХН3А
6	38ХМЮА
7	40ХН
8	35ХН1МФА
9	15Х1М1Ф
10	25Х1МФ

Table 2

Recommended modes ion beam treatment

Current, A	Vacuum, MPa	The temperature of the ion-beam treatment, ^{o}C
85	$3 \cdot 10^{-3}$	175
90	$4 \cdot 10^{-3}$	185
95	$5 \cdot 10^{-3}$	195

Table 3

The study protocol process of ion-beam treatment of surface details sample

sample material	The temperature of the ion-beam treatment, ^{o}C	Current, A	Vacuum, MPa	Proces-sing time, min	hardness details, sample IPA		corrosion resistance	
					before pro-cessing	after pro-cessing	before pro-cessing	after pro-cessing

7. CHECKLIST

7.1. What is the purpose and procedure of the job?
7.2. What types of treatment and methods of hardening of metals, you know?
7.3. Define the process of ion-beam treatment.
7.4. Specify the features and advantages of ion beam treatment.
7.5. What operations include surface preparation details before processing?
7.6. What are the basic operations of process technology of ion-beam treatment?
7.7. What factors (modes) have a decisive effect on the quality of treatment?
7.8. Describe the technique for measuring the microhardness details sample surface.

Список рекомендуемых источников

1. Попок, Н.Н. Мобильная реорганизация машиностроительного производства / Н.Н. Попок. – Минск : УП «Технопринт», 2001. – 396 с.

2. Емельянов, В.А. Вакуумно-плазменные способы формирования защитных и упрочняющих покрытий / В.А. Емельянов, И.А. Иванов, Ж.А. Мрочек ; под. общ. ред. Ж.А. Мрочека. – Минск : Изд-во НПО «Интеграл», 1998. – 284 с.

3. Прогрессивные методы изготовления металлорежущих инструментов / А.В. Белый [и др.]. – Минск : БелНИИНТИ, 1989. – 56 с.

4. ООО "ПрофиПроект" [Электронный ресурс]. – Режим доступа: http://www.profyproject.ru/iznosostoykie_pokrytiya_i_uprochnenie.

5. Ионно-лучевая обработка металлов, сплавов и керамических материалов / А.В. Белый [и др.]. – Минск : Изд-во Физ.-тех. ин-та НАН Беларуси, 1998. – 220 с.

6. ООО «Мир гальваники» [Электронный ресурс]. – Режим доступа: http://www.galvanicworld.com.

7. Попок, Н.Н. Исследование процесса ионно-лучевой обработки инструментальных материалов // Н.Н. Попок, В.А. Кукареко, С.В. Дербуш // Вестн. Полоцк. гос. ун-та. Сер. С. Фундаментальные науки. – 2008. – № 3. – С. 99–105.

8. Физические и технологические основы ионно-лучевой обработки материалов : пособие для студентов машиностроительных специальностей / А.В. Белый [и др.]. – ПГУ, 2010. – 84 с.

CONTENT

Учебное издание

ПОПОК Николай Николаевич
ДЕРБУШ Сергей Владимирович
ПОПОК Анна Николаевна

ИОННЫЕ ИСТОЧНИКИ: ВИДЫ, КОНСТРУКЦИИ, ПРИМЕНЕНИЕ

Пособие для студентов и магистрантов
машиностроительных специальностей
на английском языке

Редактор *Д. М. Севастьянова*
Дизайн обложки *И. В.Ворсовой*

Подписано в печать 20.03.2017. Формат 60×84 1/16. Бумага офсетная.
Ризография. Усл. печ. л. 4,18. Уч.-изд. л. 3,92. Тираж 30 экз. Заказ

Издатель и полиграфическое исполнение:
учреждение образования «Полоцкий государственный университет».
Свидетельство о государственной регистрации
издателя, изготовителя, распространителя печатных изданий
№ 1/305 от 22.04.2014.

ЛП № 02330/278 от 08.05.2014.

Ул. Блохина, 29, 211440, г. Новополоцк.